Published in final edited form as:

Annu Rev Biomed Eng. 2018 June 04; 20: 403–429. doi:10.1146/annurev-bioeng-062117-121113.

Physiology and Engineering of the Graded Interfaces of Musculoskeletal Junctions

Edward D. Bonnevie[1,2], **Robert L. Mauck**[1,2]

[1]McKay Orthopaedic Research Laboratory, Department of Orthopaedic Surgery, and Department of Bioengineering, University of Pennsylvania, Philadelphia, Pennsylvania 19104, USA

[2]Translational Musculoskeletal Research Center, Col. Michael J. Crescenz Veterans Administration Medical Center, Philadelphia, Pennsylvania 19104, USA

Abstract

The connective tissues of the musculoskeletal system can be grouped into fibrous, cartilaginous, and calcified tissues. While each tissue type has a distinct composition and function, the intersections between these tissues result in the formation of complex, composite, and graded junctions. The complexity of these interfaces is a critical aspect of their healthy function, but poses a significant challenge for their repair. In this review, we describe the organization and structure of complex musculoskeletal interfaces, identify emerging technologies for engineering such structures, and outline the requirements for assessing the complex nature of these tissues in the context of recapitulating their function through tissue engineering.

Keywords

gradients; interfaces; articular cartilage; tendon; bone; temporomandibular joint; intervertebral disc

1. INTRODUCTION

The joining of dissimilar materials is a universal requirement for the function of soft connective tissues. In a classical engineering context, connecting materials with differing mechanical properties and structures poses a difficult task—when dissimilar materials join and are subsequently loaded, nontrivial strain fields and stress concentrations arise at these boundaries (1). Given these areas of amplified stress and strain in such materials, the boundary between the two materials is predisposed to failure. As a simple example, consider a composite material consisting of soft and stiff regions in series with one another that is loaded in tension. Due to the large variations in mechanical properties, the deformations of the two materials will be dependent on each material's modulus and Poisson ratio. At the interface, to maintain material connectivity, stress concentrations will necessarily arise as the two materials compensate for these mismatched properties to maintain a continuous interface.

lemauck@mail.med.upenn.edu.

Such problems are of considerable interest within the field of biomechanics, as dissimilar material connections are present throughout the musculoskeletal system (Figure 1). In a simplified context, connective tissues can be grouped into fibrous, cartilaginous, and calcified (i.e., bone) tissues, and connections between all of these types are present in the body. One such example is in diarthrodial joints, in which a graded structure in articular cartilage from the articular surface evolves over the depth of the tissue until it reaches the calcified cartilage zone and then transitions to subchondral bone (2–5). At this interface, a relatively soft, proteoglycan-rich cartilage connects to a stiff, calcified bone. Similarly, dense fibrous tissues such as tendon and ligament exhibit graded mechanical structures along their long axis, most notably at their interfaces with bone (6). Mechanically mediated development of this interface culminates with the permanent inclusion of a compliant fibrocartilaginous region that serves to attenuate stress concentrations across this interface. Indeed, the toughness of the tendon/ligament entheses is attributed to this graded material inclusion (6–8). As another example, within the temporomandibular joint (TMJ), the mandibular cartilage contains a fibrous superficial zone that transitions to hyaline cartilage deeper into the tissue, and eventually to bone (9, 10). In the most complicated scenario, the intervertebral disc (IVD) contains all of the above types of material attachments (fibrous–bony, cartilaginous–bony, and fibrous–cartilaginous) (11).

Given the centrality of all of these tissues in load-bearing function across the musculoskeletal system, and their propensity for failure, each one is of considerable interest in the areas of regenerative medicine and functional tissue engineering. Additionally, failure of these tissues results in arthritis, tendinopathy, temporomandibular disorders, and back pain, all of which engender significant physical and financial burdens (12–15). Consequently, the last two decades have witnessed considerable effort toward recapitulating these structures in the lab using tissue engineering approaches. Given that the primary roles of these tissues are mechanical in nature, attempts to replicate tissue function through material design has focused on these refined mechanical attributes. Furthermore, cells that are resident in these tissues sense and respond to the local mechanical environment (16) and the emergent mechanical gradients that develop during degeneration and repair. In this review, we outline the stepwise progression in tissue engineering approaches that aim to reproduce the complexity of these interfaces, and describe the state of the art and future trajectory of this work. Furthermore, we highlight the importance of analyzing these graded structures and review the roles that two-dimensional (2D) and three-dimensional (3D) analysis techniques offer in terms of developing a comprehensive view of both native and engineered tissue. Finally, we relate the large body of research in the osteochondral and enthesis engineering fields to other soft connective tissue fields that are still developing. Specifically, we briefly review the current state of TMJ condylar cartilage engineering, which seeks to produce a tissue with the unique structure of a fibrous superficial zone that connects to hyaline cartilage in the deeper regions of the tissue, and we address the rapidly growing field of IVD tissue engineering. The disc exhibits graded material connections of all of the mentioned forms above; cartilaginous tissue meets bone where the nucleus pulposus (NP) and cartilaginous end plate meet the vertebra, fibrous tissue connects to bone where the annulus fibrosus (AF) meets the vertebra, and cartilaginous tissue connects to fibrous tissue where the NP meets the AF. Thus, this tissue represents the holy grail of interface

engineering, and the solution to each one of these interfaces will have a broad impact across the field.

2. ENGINEERING THE GRADED STRUCTURE OF ARTICULAR CARTILAGE

2.1. Graded Cartilage Structure and Function

Articular cartilage is one of the most unique naturally occurring materials. Its capacity to carry stresses that far exceed its equilibrium modulus, over millions of cycles, is a characteristic not found in any human-made material. This unique function is tied heavily to the composite, graded structure of the tissue. Organized type II collagen fibers provide scaffolding that is stiff in tension but easily compressed (17, 18). This fibrous network is interdigitated by sulfate-rich proteoglycans, specifically aggrecan. Negative charges on these proteoglycans contribute a high fixed charge density to the tissue and substantially increase the osmotic potential of the tissue, and the resulting Donnan osmotic pressures in the tissue can readily surpass 100 kPa (19, 20). Interspersed in this highly hydrated matrix, the resident chondrocytes slowly turn over and renew the extracellular matrix (ECM).

While the above description captures the tissue at the bulk level, its structure and function vary through the depth of the tissue, from the articular surface to the subchondral bone (Figure 2). At the articular surface, the structure of cartilage adopts a structure that is highly efficient in load bearing. In this superficial zone, type II collagen fibers are aligned perpendicularly to the articular surface (2, 21). This fibrous makeup provides a high tensile modulus that limits lateral, or Poisson, expansion under axial loading. Additionally, whereas aggrecan content is low in this zone, another proteoglycan provides functional properties. Lubricin, or proteoglycan 4, is secreted by the elongated superficial zone chondrocytes, attaches to the articular surface, and lubricates the interface between two opposing cartilage surfaces (22–24). The combination of low hydraulic permeability, high tensile modulus, and lubricating macromolecules results in articular cartilage having some of the lowest naturally occurring coefficients of friction found in nature. On a level deeper than the articular surface in the middle zone, chondrocytes adopt a rounded morphology and produce substantial amounts of aggrecan as well as randomly oriented type II collagen. Beyond the middle zone, away from the articular surface, the deep zone of cartilage shows collagen that is predominantly oriented perpendicularly to the subchondral bone interface (21), where a mineralization gradient extends from calcified cartilage at the tide mark and into the subchondral bone (5).

This variation in cartilage structure and organization dictates a corresponding gradient in the mechanical properties of the tissue (25, 26). Both compressive and shear stiffness increase nearly monotonically from the articular surface through the subchondral bone. However, tensile properties exhibit the inverse relationship, decreasing as a function of tissue depth prior to reaching the mineralized zone (27). Within the mineralization gradient, the modulus varies locally on the basis of the degree of mineralization, and at the nanoscale, the modulus can surpass 30 GPa (5). This graded structure ensures proper cartilage function, as the superficial zone shields the deep regions of tissue from elevated strains by dissipating energy and serving as a strain sink (28, 29).

2.2. Alterations of Structure in Degeneration and Disease

The functionally graded structure described above can change markedly in the context of injury, aging, and cartilage degradation (Figure 2c,d). Hallmarks of early osteoarthritis are decreased cellularity within the superficial zone and decreased proteoglycan content in a progressively expanding front that extends from the articular surface (30). This phenomenon of altered structure in the context of degeneration has been qualitatively evaluated for decades using histological techniques; however, recent advances in spectroscopy have enabled a more quantitative analysis of this spatially varying graded structure in the context of degeneration (31, 32). As cartilage degradation progresses, the articular cartilage softens in concert with stiffening of the subchondral bone (33, 34). These changes alter the load-bearing capabilities of articular cartilage, resulting in further damage and degeneration. For this reason, it is imperative that tissue engineering approaches to restore cartilage function fully recapitulate the native, healthy graded structure of this tissue.

2.3. Tissue Engineering for Articular Cartilage Repair

Tissue engineering approaches in regenerative medicine seek to repair or replace damaged or degenerated tissue with lab-grown constructs (35). Within tissue engineering, articular cartilage emerges as a strategic target. The lack of innervation and vascularization in mature tissue provides a simplified template in terms of implantation; however, the low levels of matrix turnover make mechanically stable integration of implanted tissue a significant hurdle (36). For this reason, among others, engineering articular cartilage that mimics the natural graded structure, including the osteochondral interface, has emerged as a focal point within the tissue engineering field. In the following sections, we review fabrication methods that seek to establish graded cartilage tissue and osteochondral interfaces via a combination of cell source and manipulation, scaffold material selection, chemical stimulus, and mechanical stimulus.

2.3.1. Cell source in osteochondral tissue engineering.—The nature of the cell source is one tool leveraged to recapitulate the graded cartilage structure within an engineered tissue. For example, in a seminal study (37), superficial and middle zone chondrocytes were selectively isolated and subsequently seeded either alone or in apposed coculture. Results from this study showed that whereas middle zone cells were superior in glycosaminoglycan (GAG) and collagen deposition within constructs, superficial zone chondrocytes produced significantly more superficial zone protein (i.e., lubricin) (37). These findings suggest that there is some degree of phenotypic maintenance of chondrocytes in 3D culture and that these distinct cell types can be harnessed to fabricate tissues with depth-dependent features (38–41). Note, however, that, for clinical translation, the availability of primary chondrocytes is limited due to the low cellular density of the native tissue. Furthermore, although expansion of chondrocytes is possible in 2D culture, the stability of the chondrocyte phenotype following 2D expansion may be compromised (42). For example, by passage 4, superficial zone chondrocytes no longer exceed deep/middle zone chondrocytes in terms of gene expression of PRG4 (43). Due to these limitations in utilizing isolated chondrocytes, stem/progenitor cells have emerged in the past decade as a viable alternative cell source in osteochondral tissue engineering (44, 45). Both bone marrow–derived and adipose-derived progenitor cells can differentiate along chondrogenic and

osteogenic lineages. Consequently, significant effort has been expended in developing culture systems that enable spatial differentiation of progenitor cells to mimic the graded structure of the osteochondral interface (38, 46). However, these cell types suffer from both the inconsistent and transient nature of their differentiation; chondrogenically differentiated stem cells commonly undergo hypertrophy and eventual ossification postimplantation (47, 48). Indeed, even when carefully engineered cartilage segments produced from stratified chondrocyte subpopulations were implanted in vivo, they did not maintain their spatially organized phenotypic characteristics, likely due to interactions with host cells (49). This finding may suggest that relying solely on cell-generated tissue constructs will be insufficient for maintaining the complex architecture of the native tissue postimplantation.

2.3.2. Graded and composite scaffold systems.—Another approach is to construct material systems that can, by design, dictate zonal organization of an engineered system while enforcing the phenotype of resident cells. These scaffold-based systems for osteochondral tissue engineering can be divided into several categories: natural scaffolds, synthetic scaffolds, scaffold-free formulations, or a combination of these groups. In seminal research by Schaefer et al. (50), cartilage and bone segments were fabricated from poly(glycolic acid) meshes and poly(lactic-*co*-glycolic acid) (PLGA) foams, respectively. Following culture, samples were combined to form an osteochondral construct. Although this study revealed early insights into how apposed culture can stimulate integration, it was unclear whether the integration of the separate parts would withstand in vivo conditions. Since that time, more sophisticated systems have been presented that enable one to dictate material gradients through the depth, for example, by sequential or graded photocrosslinking of a hydrogel (Figure 3a) (51) or additive manufacturing (i.e., 3D printing) methods (52). These techniques may address this issue of bone–cartilage integration with a defined transition region manufactured and established during a preculture period. In early research, Sherwood et al. (52) described a 3D printing technique to spatially vary material composition, porosity, and mechanics to define cartilage and bone niches prior to cell seeding. For cartilage, they fabricated a soft, 90%-porous PLGA/poly(D,L-lactic acid) material that transitioned to a 55%-porous PLGA/tricalcium phosphate material. Although this scaffold was able to mimic the mechanics of osteochondral tissue in vitro, the in vivo performance of this formulation remains to be determined. In fact, until recently it was unknown how an engineered implant would survive and remodel within the joint environment after long periods. Many studies have shown histologic differences between bone and cartilage in composite material systems both in vitro and in vivo, but it is unclear whether functional grading of cartilage occurs following implantation (53–57). Recently, Griffin et al. (58) showed that tissue-engineered cartilage implanted in an equine model for 53 weeks maintained bulk compressive properties that approached native values; however, and most strikingly, the depth-dependent shear modulus of retrieved implants revealed little to no depth-dependent remodeling, and globally the shear modulus was lower compared with that of native tissue. This finding demonstrates that the chemical and mechanical cues in the joint environment alone may not be sufficient to stimulate implanted tissue remodeling to mimic the graded structure of healthy cartilage.

2.3.3. Defined chemical cues.—Introducing chemical cues (Figure 3b), and gradients or spatial variations of these cues, has emerged as another potent regulator of matrix production and cell phenotype (56, 59–62). One way to establish these gradients is by utilizing perfusion bioreactors to induce soluble signal gradients (63). Grayson et al. (61) utilized a composite scaffold system consisting of a decellularized bone template connected to an agarose construct to promote cartilage formation. By biasing media perfusion through the bone segment of the construct, these authors showed enhanced integration of cartilage to bone, but also observed decreased chondrogenesis and cartilage matrix deposition. Growth factor gradients have also been accomplished by controlled release of soluble factors from microspheres. In an interesting study, gradients of bone morphogenetic protein 2 for osteogenesis and insulin-like growth factor 1 for chondrogenesis were developed through controlled release of these factors from PLGA–silk fibroin microspheres embedded in alginate gels (Figure 3b) (59). Note that the use of microspheres enables both spatial and temporal gradients to develop. Additionally, both material and chemical gradients can be developed simultaneously to promote the formation of functional tissue gradients (60).

2.3.4. Technologies to evaluate depth-dependent properties.—A central goal of the above studies is the development of functional cartilage tissue that exhibits native-like organization—that is, a graded structure with seamless integration with underlying bone, and recapitulation of the depth-dependent mechanical properties of the cartilage itself. In order to fully evaluate this depth-dependent variation in mechanical properties, it is not sufficient to test a construct in compression and measure a single mechanical output; this represents the average mechanics across the depth and does not provide information regarding local features. Consequently, microscopy-based strain mapping has emerged as a tool to determine the depth-dependent variation of properties (3, 4, 25, 64). In order to conduct this analysis, tissue is imaged in both free swelling and deformed states (Figure 3c), and local deformations are measured on the basis of the tracking of fiducial markers or texture using tools such as digital image correlation (29). This deformation tracking enables calculations of local deformation gradients and strain across the region of interest. In an early example of this approach, Klein et al. (3) assessed emergent depth-dependent compressive moduli in both developing native and engineered cartilage compression on a fluorescent microscope. Kelly et al. (65) used this method to show that central regions of engineered cartilage develop more slowly than the outer regions, and Farrell et al. (66) used it to show that stem cells (compared with chondrocytes) are less efficient at producing matrix in regions of limited nutrient supply. Griffin et al. (58) used similar methodology to show that, even after 53 weeks of implantation, MACI® grafts did not recapitulate the depth-dependent shear moduli of native cartilage as assessed through digital image correlation conducted on a confocal microscope. Note, however, that whereas this analysis technique may be sensitive to variations in mechanical properties of cartilage, it is relatively insensitive to variations in bone properties due to the small strains within the bone during normal loading. Additional techniques such as nanoindentation are required to evaluate the spatially varying mechanical properties of such stiff materials, including bone and mineralizing cartilage, at these important interfaces (5, 67, 68).

In addition to local assessment of mechanics, spectroscopic methods have emerged as a tool to semiquantitatively evaluate the graded biochemical structure of both native and engineered tissue. Microscope-based techniques such as Fourier transform IR (FTIR) spectroscopy (32, 69, 70) and Raman spectroscopy (71) enable evaluation of biochemical gradients in either fixed or hydrated tissues (Figure 3d). While these analysis techniques have been used widely to determine the evolution of cartilage structure in the context of health and degeneration (32), they can also provide important information about the development of heterogeneity in engineered tissue. Kim et al. (69) proposed the use of FTIR spectroscopy as a quantitative tool to measure the spatial variations of proteoglycan content within tissue-engineered constructs by deconvolution of amide peaks. Furthermore, a recent study by Bergholt et al. (72) investigated the depth-dependent biochemical makeup of both native and tissue-engineered cartilage using Raman spectroscopy. In native tissue, imaging followed by deconvolution of the signal on a pixel-by-pixel basis enabled 2D mapping of the tissue structure. In hydrated tissue, this signal can be separated to reveal trends in collagen concentration and orientation, GAG concentration, mineral content, water content, and cellularity (72). This recent study revealed depth dependence in collagen, GAG, and water content, which have been independently connected to local mechanics within engineered cartilage constructs (3, 73).

Looking toward the future of articular cartilage tissue engineering, we envision that techniques such as microscope-based strain mapping and biochemical analysis will find use as nondestructive tools that can be implemented prior to implantation of an osteochondral construct. In the near future, these techniques could be coupled with in vivo studies to analyze (*a*) how defined graded structures translate to in vivo tissue performance and (*b*) how in vivo conditioning and maturation may promote or inhibit functional remodeling of such constructs. Ultimately, the restoration of this graded function, from superficial zone to subchondral bone, will be essential for durable cartilage repair.

3. ENGINEERING TENDON AND LIGAMENT ENTHESES

3.1. Graded Enthesis Structure and Function

The insertions that tendons and ligaments make to bone are another natural example of function dictated by a composite, graded structure (Figure 4). Aligned, fibrous tendons and ligaments attach to stiff, calcified bone via an intermediate fibrocartilaginous region. This region can be thought of as a stress or strain dissipater that inhibits the formation of stress and strain concentrations at the interface of fibrous tissue and bone. In this partially mineralized region, the collagen fiber angle distribution is more disperse than in the tendon midsubstance, and consequently, this region is more compliant (74,75). This fibrocartilage region is pivotal in establishing the failure energy (i.e., toughness) of the tendon-to-bone interface. Recent experimental evidence revealed that increased compliance of this fibrocartilaginous region does not scale universally with mineral content and that, on the microscale, the toughness of the insertion far exceeds the toughness measured on the macroscale (8). While this fibrocartilaginous inclusion contains lower collagen content and higher proteoglycan content than the fibrous midsubstance, it also exhibits a transition from type I to type II collagen (76, 77). Consequently, in the context of regeneration and repair,

the replication of this tough, compliant zone may be essential for ensuring proper tendon and ligament function.

3.2. Injury and Repair of Fibrous Insertions

Tendon injuries do not typically occur in the midsubstance of the tissue. Most commonly, overloading or fatigue of the tissue culminates in disruption of the musculotendinous junction, where muscle meets tendon, or the osteotendinous junction, where tendon meets bone (78–80). Healing of injured tendon or ligament is characterized by the formation or deposition of scarlike fibrous tissue at this interface. Given the disorganization of this repair tissue, and the lack of stratified transitional zones, the toughness of the native enthesis is rarely reproduced (81), predisposing this junction to reinjury and further degeneration. Typically, tendon healing following injury shows a time-dependent evolution in stiffness as the tissue transitions from the inflammatory to the proliferative to the remodeling phase. Even after remodeling and maturation, however, repaired tendon insertions do not reach native, healthy mechanical properties (81), which may be due, in part, to the fact that treatment strategies to repair this junction via bone tunnels do not provide ideal mechanical support in the early stages of healing (82). Alternatively, because the original junction is precisely established over the course of development (83–85), it may be that the natural sequence of cell type and fate transitions simply cannot be recapitulated in the context of wound repair in the adult.

3.3. Tissue Engineering for Tendon and Ligament Repair

Due to the poor healing of tendon and ligament and their attachments, tissue engineering approaches to repair and regenerate this interface have been of considerable interest. For the sake of conciseness, we focus on the formation and analysis of functionally graded tissue. For a more complete overview of the general field of tendon and ligament tissue engineering, the reader is directed to several recent reviews that also address this broader topic (86, 87).

3.3.1. Cell sources for enthesis engineering.—As with most tissue engineering approaches, a major question in the preliminary stages of forming functional tissue is that of the source of cells to be utilized. Similar to cartilage tissue engineering, both differentiated and progenitor cell populations provide viable sources (88). Additionally, recent evidence suggests that priming progenitor cells toward a tenogenic phenotype by inducing scleraxis overexpression might functionally enhance progenitor cell populations for tendon-related tissue engineering (89). This finding is of interest in the context of this review, as scleraxis expression is necessary for the formation of a functional enthesis structure (85).

3.3.2. Organized fibrous scaffolds for enthesis engineering.—A hallmark of the tendon and ligament midsubstance is its aligned, organized, and fibrous composition. Because this structure imparts the high tensile modulus into the tissue, considerable effort has been devoted to developing aligned fibrous scaffolds for tissue engineering purposes. Here, we focus on two methods of developing this mechanical anisotropy in scaffolds: electrospinning of natural and synthetic polymeric materials and alignment of natural scaffold materials through cell-generated traction forces.

Over the past several decades, electrospinning technologies have become a standard method for producing aligned, anisotropic polymeric scaffolds (90). Electrospinning involves the charging of a polymeric solution until such time that charge–charge interactions in the solution overcome the surface tension of that solution. At this point, a fine stream is emitted from the solution (spinneret), and transits rapidly to the nearest grounded surface (collector). The versatility of this scaffold fabrication method is highlighted by the independent control of fiber organization, diameter, and stiffness through such controllable variables as rotation speed of the collector, voltage potential and distance between spinneret and collector, and material choice, respectively. For example, tuning the surface speed of the rotating collection mandrel from 0 m/s to 9 m/s enables the formation of nonaligned fiber networks and highly aligned networks from the same material (Figure 5a) (91). Additionally, the choice of material allows for independent tuning of overall scaffold stiffness. For example, a scaffold fabricated by spinning poly(ε-caprolactone) (PCL), compared with a scaffold consisting of PLGA, can exhibit tensile moduli more than an order of magnitude lower, independent of fiber morphology (91–93). Substantial emphasis has also been placed on developing aligned scaffolds based on natural materials. Silk (silk fibroin) (94), gelatin (95), hyaluronic acid (96), and collagen (97) are only a few examples of natural materials that can be readily formed into fibers. Additionally, composite materials containing both synthetic and natural polymers can be fabricated to tune both degradation kinetics and presentation of cellular cues (e.g., PCL and collagen) (98).

In addition to alignment of fibrous environments through collection on rotating mandrels, cellular traction forces and material remodeling can be harnessed to develop aligned fibrous tissues (Figure 5b). This method is most commonly applied in collagen gels, which are particularly relevant for tendons and ligaments because type I collagen is the primary structural protein. Often, fibroblasts or similarly contractile cell types (e.g., mesenchymal stem cells) are embedded within a low-density collagen matrix, and over time, these cells exert traction forces against the material (and deposit new matrix) to compact it into a denser structure (99, 100). By manipulating the boundary conditions against which this contraction occurs, one can direct the alignment in a particular direction, forming a dense, organized, fibrous tissue (101). This cell-mediated contraction also results in significant stiffening of the structure, reaching levels well over an order of magnitude stiffer than the starting material (100–102).

3.3.3. Development of composite and graded structures in fibrous tissue engineering.—While the above methods provide a means to replicate the midsubstance of tendons and ligaments, additional innovation has focused on the development of functionally graded insertions. Such transition points are required because these fibrous tissues must form strong attachments to bone that are not predisposed to failure. To mimic this transition, several techniques have been reported that can foster the mineralization of both native and engineered tissue. For instance, Li et al. (103) fabricated a mineralization gradient along the axis of a fibrous scaffold (Figure 5c). They did so by slowly immersing an electrospun scaffold into a mineralizing solution containing calcium phosphate. The gradient of mineralization that formed along the scaffold occurred in a manner that was proportional to immersion time (Figure 5c). Taking a different approach, Erisken et al. (104) incorporated

mineralization into the electrospinning process itself. They developed a system in which PCL was electrospun from two sources, with polymer containing calcium phosphate first deposited on the bottom surface and PCL alone deposited last, forming the top layer. As opposed to these methods using mineralized synthetic scaffolds, Phillips et al. (105) tuned the local differentiation of fibroblasts in collagen matrices to promote regional mineralizing activity. They accomplished this task by immobilizing viral vectors delivering pro-osteogenic transcription factors (i.e., Runx2/Cbfa1) along the material itself. By providing these chemical cues in a graded manner, these authors developed a cell-mediated mineralization gradient. More recently, other mineralization techniques have been presented. For example, Smith et al. (106) described multiple modes of mineralization of collagen scaffolds that were associated with varying degrees of toughness.

3.3.4. Assessing graded structures in engineered entheses.—

As was the case with engineering the graded structure in articular cartilage, developing the desired mechanical profile within an engineered enthesis is a primary goal. Although methods to incorporate mineralization into natural and synthetic scaffolds have been developed, few studies have reported the functional consequences of such mineralization. Local mineral quantification based on spectroscopic or computed tomography scanning techniques can provide estimates of the functional changes that occur due to mineralization. However, more direct methods, such as strain mapping, are indispensable for evaluating the mechanical consequences of this altered mineral structure. To that end, an early report of mineralization gradients coupled mineral measurements with texture-based strain mapping to demonstrate a correlative relationship between mineral content and local modulus (Figure 5c) (103). Furthermore, the same research group recently reported a more robust and less computationally demanding method to extract local strains (and, consequently, stiffnesses or moduli) that determines deformations directly on the basis of image correlation with an included warping function (107). Such analysis techniques will be essential for fine-tuning the gradation of mineralization to develop a tissue-engineered enthesis that stress shields in a manner similar to the native structure.

4. ENGINEERING FIBROUS TO CARTILAGINOUS MATERIAL CONNECTIONS

4.1. Natural Structure of the Mandibular Condyle

In addition to the importance of cartilaginous-to-bone and fibrous-to-bone connections, other structures throughout the musculoskeletal system show less common but equally important transitions in tissue types. The cartilage of the mandibular condyle is one such example, with zonal characteristics that contrast markedly with those of typical articular cartilage (Figure 6). Specifically, the mandibular cartilage possesses a predominant fibrous superficial zone composed of type I collagen that is more reminiscent of the aligned collagenous structures one would see in fibrous tissues such as tendon and ligament than the thin superficial zone of articular cartilage (108–110). This fibrous superficial zone connects to middle to deep cartilaginous regions that are typically grouped into proliferative, mature, and hypertrophic regions and, in a graded fashion, connects the fibrous zone and the underlying hyaline-like cartilage.

Despite the differences in structure from hyaline cartilage, the TMJ condylar cartilage exhibits degenerative changes consistent with whole-joint osteoarthrosis (14, 113). Because of the relatively high prevalence of TMJ disorders, considerable effort has focused on the restoration of function in this critical joint (114, 115). Although numerous studies have attempted to engineer a TMJ disc replacement, analogous to the meniscus of the knee, that work is not the focus of this article, and the reader is referred to several reviews on that topic (116, 117). Instead, we focus here on the unique transition of fibrous to cartilage tissue within the TMJ condylar cartilage.

To understand the metrics for successful TMJ condyle tissue engineering, one must first understand the role that its unique structure plays in dictating the proper function of the condyle. The TMJ cartilage maintains similar lubricating capacity as articular cartilage in other diarthrodial joints (118, 119). In both types of cartilage, tension–compression nonlinearity is a critical feature that enables load bearing and lubrication. That is, due to significantly higher tensile stiffness compared with compressive stiffness, the ability to pressurize interstitial fluid is enhanced, leading to enhanced load support and reduced frictional forces (120, 121). Within the TMJ mandibular cartilage, this tension–compression nonlinearity is even more apparent than in hyaline cartilage (10), due to the thickened fibrous layer (Figure 6e). Indeed, on the basis of theoretical models, it has been hypothesized that this superficial zone shields the underlying cartilaginous tissue and bone from excessive loading and promotes more effective lubrication (Figure 6b) (9). Given the complex loading environment of the TMJ, recapitulating this graded, composite fibrous–cartilaginous structure in engineered tissue may be essential for ensuring the function and longevity of any engineered replacement.

4.2. Progress and Challenges in Engineering Temporomandibular Joint Cartilage

Due to the prevalence of symptomatic TMJ disorders and arthroses, investigators have devoted considerable effort to engineering replacement tissues (115). As noted above, the graded structure of TMJ cartilage contains fibrous–cartilaginous interfaces in addition to cartilaginous–bony attachments. For the sake of conciseness, we do not discuss the cartilage–bone connection here, and we refer the reader to the above section on osteochondral interfaces in articular cartilage, as well as to several seminal papers on this topic (122–124).

As in the case of articular cartilage, one of the primary obstacles in engineering effective replacements for the TMJ condylar cartilage is the development of a robust cartilage–bone connection. However, unlike most of the articular cartilage research that focuses on constructs that can fill a small defect, TMJ tissue engineering more commonly seeks to replace the entire mandibular condyle. In cases of craniofacial trauma, reconstructive surgery may require the inclusion of both the articular cartilage and substantial sections of the mandible (125). For this reason, 3D printing techniques have been utilized to develop large sections of the mandible with an integrated engineered cartilage construct on the condylar surface (Figure 6f). As described in detail above, and following similar trends, there have been substantial research efforts toward the formation of the bone–cartilage

interface via variation in material choice, cell source, and chemical stimulus (Figure 6f) (115).

Because loading patterns for the TMJ vary greatly compared with other diarthrodial joints and the inclusion of the fibrous superficial layer enhances load-bearing properties, it is unclear whether simply recapitulating the cartilaginous and bone components will be sufficient to restore proper function. Thus, an open question remains concerning how to engineer an integrated, fibrous, superficial zone that shields the underlying cartilage and bone during activities such as chewing, biting, and talking. Technologies incorporating principles of both cartilaginous and fibrous tissue engineering may need to be unified to produce a functional replacement for this unique interface.

5. ENGINEERING THE INTERVERTEBRAL DISC

5.1. Native Disc Structure and Function

IVDs enable mobility of the spine. They connect adjacent vertebrae and allow six degrees of freedom in movement. This function relies heavily on the composite structure of the healthy disc. An inner, gel-like NP region maintains substantial swelling pressures due to a high fixed charge density. This osmotic swelling is due to high proteoglycan concentrations and can readily surpass 100 kPa (126, 127). This inner region is laterally confined by the AF, which both connects adjacent vertebrae and restricts the radial swelling of the NP. The AF consists of a fibrous, lamellar structure that is dominated by type I collagen organized into alternating orientations of ±30° to the coronal plane in adjacent lamellae (128). The NP connects to an underlying cartilaginous end plate connecting the NP to bone (129), whereas the AF connects directly to the vertebrae. In short, the IVD exhibits a composite structure across different length scales and includes multiple types of material connections (Figure 7).

In the context of degeneration, NP swelling decreases as proteoglycan content falls, and the disc height decreases markedly with loss of swelling pressure (127). Such degenerative changes in the disc are closely linked to increased incidence of low back pain (131). Although back pain is a leading cause of disability (13), the field of whole-disc tissue engineering is immature compared with the fields of tendon and cartilage tissue engineering. Here, we assess several techniques that show promise in recapitulating the composite structure of the IVD that seek to recapitulate the gradients in composition and stiffness and multiple material interfaces that occur over more than one axis of the tissue and are required for its mature function.

5.2. Development of Composite, Engineered Intervertebral Disc Constructs

To date, several groups have developed and implanted tissue-engineered, composite structures in small animal/rodent models with varying degrees of success. To fully appreciate the obstacles that must be overcome when implanting a whole tissue-engineered IVD, however, we first assess significant advances in engineering the AF and NP individually, and then explore how these discrete elements can be combined.

5.2.1. Annulus fibrosus tissue engineering.—AF cells can adhere to, proliferate on, and deposit ECM in a variety of natural and synthetic biomaterials (132–135). However,

maintenance of an elongated cell shape within an organized anisotropic fibrous matrix (i.e., the microstructure and cell morphology of the native AF) cannot be accomplished in all engineered environments. Consistent with the above discussion of tendon and ligament tissue engineering, electrospinning of natural or synthetic materials has emerged as a promising tool to develop this desired microenvironment (136, 137). Cells seeded into such engineered environments deposit an aligned collagen-rich ECM that can stiffen constructs to near-native levels in term of linear modulus (136).

Despite the promise in developing near-native mechanics within single lamellae sheets, it is important to note that the AF consists of multiple sheets arranged in alternating fiber orientations. These organized lamellae are important for establishing the complex mechanics of the native tissue that serve the dual purpose of confining NP expansion and maintaining vertebral body connection. One study effectively recapitulated this structural hierarchy through an apposed culture of aligned fibrous sheets with alternating ±30° orientations (Figure 8a). In fact, maturation of these constructs facilitated deposition of an interlamellar matrix that elevated mechanical properties closer to native levels than apposed sheets with parallel orientations (137).

5.2.2. Nucleus pulposus tissue engineering.—The NP poses similar challenges to tissue engineering as articular cartilage (described above). One of the obstacles in forming effective NP tissue is maintaining a stable NP-like phenotype. To this end, biomaterials have been developed that provide specific cellular cues that can tune matrix production by embedded or encapsulated cells toward an NP-phenotype rich in type II collagen and proteoglycan. In contrast to articular cartilage, though, the ratio of proteoglycan to collagen is significantly higher in the NP (139), and the tissue exhibits both fluid- and solid-like mechanics (140). In one study, NP cells seeded on a calcium polyphosphate substrate produced significant amounts of proteoglycans but did not produce substantial collagen (141). As a result, constructs approached native NP equilibrium mechanical properties, but the dynamic shear properties fell short of native levels. To address this limitation, a number of studies have sought to optimize methods for cell seeding/encapsulation (142, 143), cell source (144, 145), and chemical cues (146, 147) to promote the NP-like phenotype. However, although these methodologies can begin to replicate the form and function of explanted NP tissue, the IVD must function as a whole where composite mechanics dictate proper in vivo function.

5.2.3. Composite nucleus pulposus–annulus fibrosus structures.—Due to the inherent complexity of assembling a fibrous and cartilaginous composite structure that must then integrate with the native environment postimplantation, tissue engineering of a complete IVD poses a challenge. To date, methods that seek to fabricate this composite structure have utilized tools and techniques similar to those described above (148–151). Mizuno et al. (148, 149) first described a method to develop a composite IVD by surrounding an engineered NP formed by cells encapsulated in alginate by an AF cell-seeded synthetic polymer foam. In a subsequent elegant study by Bowles et al. (152), cell-mediated collagen compaction (Figure 8b) was used to assemble a circular fibrous AF around an NP hydrogel. By allowing collagen to contract around a central gel, cells adopted

an elongated, fibroblast-like phenotype. These cells, through a combination of matrix deposition and reorganization, developed a circumferentially aligned AF that significantly enhanced the mechanical properties of the composite. A follow-up study, which included in vivo implantation, demonstrated the ability of these tissue-engineered discs to maintain hydration and disc height following implantation in a rat caudal disc model (153). Recently, this process has shown promise in replacing canine cervical discs (138).

One aspect of the native disc structure missing from the above-described study is development of the lamellar nature of the AF with alternating fiber angles of adjacent lamellae. Just as electrospinning has emerged as a useful tool to develop aligned fibrous tissue for tendon and ligament, this technique can be implemented to form the lamellar AF structure prior to combination with an NP material. Nerurkar et al. showed that the combination of the lamellar AF structure described above with a hydrogel NP region could significantly enhance the mechanical properties of an engineered disc (Figure 8a) (150). As these engineered discs are compressed, the lateral expansion of the NP engages the fibers of the AF. Due to the intrinsically high modulus of the electrospun fibers (PCL), the engineered AF effectively restricts lateral disc expansion in a similar manner to the native disc. Follow-up studies including in vivo implantation revealed the ability of these discs to maintain vertebral body separation; however, the proteoglycan-rich nature of the preimplantation NP was not conserved (154, 155).

The loss of NP proteoglycan revealed by Martin et al. (155) highlights an opportunity to enhance IVD composite tissue engineering—the inclusion of a cartilaginous end plate (129). In cases where disc replacement has become an option to restore spine mechanics, it is more than likely that degenerative changes to the cartilaginous end plates have occurred in tandem with AF and NP degeneration (156). With this in mind, it is likely that a suitable IVD replacement will include this structure to restore proper function of the disc and maintain attachments to the apposed vertebrae. Additionally, incorporation of the end-plate structures may serve as a barrier to host cell infiltration from the surrounding environment, a possible route through which fibrotic remodeling of the implanted NP occurs. Recent evidence suggests that such a strategy may be effective, as incorporation of end plate–like structures mitigates in vivo proteoglycan loss (157).

6. CONCLUSIONS

We have presented a brief overview of four interrelated fields that all seek to achieve a similar task: replicating the composite, graded structures of connective tissues and their connections with one another. In doing so, we have highlighted key technologies developed within the cartilage and tendon/ligament fields and provided insight into how these technologies can be harnessed to rapidly progress the less developed fields of TMJ and IVD tissue engineering. As these fields develop, and more complexity is embedded within these engineered tissues, the use of quantitative 2D and 3D analysis techniques will prove necessary to map the complexity of emergent mechanical properties, especially at the interfaces between tissue types. In order to fully appreciate how the elements of composite structures interact, spatial mapping of both the biochemical content and mechanics will be required to reveal areas of weakness and the need for further refinement. Understanding the

shortcomings of an engineered tissue not only can reveal why such a construct did not work perfectly but also will likely provide direction for new strategies to develop more effective tissues.

The incorporation of such material stiffness gradients for the purpose of producing functional musculoskeletal tissues requires consideration of how cells sense and respond to their local mechanical microenvironments. It is increasingly well understood that cells respond to the stiffness of their local environment, and that this cellular mechanical input can guide adoption and/or retention of phenotype (158). Future studies in this area will need to more fully explore how the gradients that define tissue connections influence function at the cellular length scale, and how these cues may be leveraged to facilitate more effective tissue-engineered endeavors that mimic graded native microenvironments (159).

ACKNOWLEDGMENTS

The authors gratefully acknowledge support from the National Institutes of Health (T32 AR53461-11, R01 EB02425, and P30 AR050950) and the US Department of Veterans Affairs (I01 RX002274).

DISCLOSURE STATEMENT

The authors are not aware of any memberships, affiliations, funding, or financial holdings that might be perceived as affecting the objectivity of this review.

LITERATURE CITED

1. Delale F 1984 Stress singularities in bonded anisotropic materials. Int. J. Solids Struct. 20:31–40
2. Jeffery AK, Blunn GW, Archer CW, Bentley G. 1991 Three-dimensional collagen architecture in bovine articular cartilage. J. Bone Joint Surg. Br. 73:795–801 [PubMed: 1894669]
3. Klein TJ, Chaudhry M, Bae WC, Sah RL. 2007 Depth-dependent biomechanical and biochemical properties of fetal, newborn, and tissue-engineered articular cartilage. J. Biomech. 40:182–90 [PubMed: 16387310]
4. Buckley MR, Gleghorn JP, Bonassar LJ, Cohen I. 2008 Mapping the depth dependence of shear properties in articular cartilage. J. Biomech. 41:2430–37 [PubMed: 18619596]
5. Ferguson VL, Bushby AJ, Boyde A. 2003 Nanomechanical properties and mineral concentration in articular calcified cartilage and subchondral bone. J. Anat. 203:191–202 [PubMed: 12924819]
6. Liu Y, Birman V, Chen C, Thomopoulos S, Genin GM. 2011 Mechanisms of bimaterial attachment at the interface of tendon to bone. J. Eng. Mater. Technol. 133:011006 [PubMed: 21743758]
7. Thomopoulos S, Birman V, Genin GM. 2013 The challenge of attaching dissimilar materials In Structural Interfaces and Attachments in Biology, pp. 3–17. New York: Springer
8. Deymier AC, An Y, Boyle JJ, Schwartz AG, Birman V, et al. 2017 Micro-mechanical properties of the tendon-to-bone attachment. Acta Biomater. 56:25–35 [PubMed: 28088669]
9. Ruggiero L, Zimmerman BK, Park M, Han L, Wang L, et al. 2015 Roles of the fibrous superficial zone in the mechanical behavior of TMJ condylar cartilage. Ann. Biomed. Eng. 43:2652–62 [PubMed: 25893511]
10. Singh M, Detamore MS. 2008 Tensile properties of the mandibular condylar cartilage. J. Biomech. Eng. 130:011009 [PubMed: 18298185]
11. Nerurkar NL, Elliott DM, Mauck RL. 2010 Mechanical design criteria for intervertebral disc tissue engineering. J. Biomech. 43:1017–30 [PubMed: 20080239]
12. Cross M, Smith E, Hoy D, Nolte S, Ackerman I, et al. 2014 The global burden of hip and knee osteoarthritis: estimates from the Global Burden of Disease 2010 study. Ann. Rheum. Dis. 73:1323–30 [PubMed: 24553908]

13. Buchbinder R, Blyth FM, March LM, Brooks P, Woolf AD, Hoy DG. 2013 Placing the global burden of low back pain in context. Best Pract. Res. Clin. Rheumatol. 27:575–89 [PubMed: 24315140]
14. Tanaka E, Detamore MS, Mercuri LG. 2008 Degenerative disorders of the temporomandibular joint: etiology, diagnosis, and treatment. J. Dent. Res. 87:296–307 [PubMed: 18362309]
15. Sharma P 2005 Tendon injury and tendinopathy: healing and repair. J. Bone Jt. Surg. 87:187–202
16. Buxboim A, Rajagopal K, Brown A, Discher DE. 2010 How deeply cells feel: methods for thin gels. J. Phys. Condens. Matter 22:194116 [PubMed: 20454525]
17. Huang C-Y, Soltz MA, Kopacz M, Mow VC, Ateshian GA. 2003 Experimental verification of the roles of intrinsic matrix viscoelasticity and tension–compression nonlinearity in the biphasic response of cartilage. J. Biomech. Eng. 125:84–93 [PubMed: 12661200]
18. Soltz MA, Ateshian GA. 2000 A conewise linear elasticity mixture model for the analysis of tension-compression nonlinearity in articular cartilage. J. Biomech. Eng. 122:576–86 [PubMed: 11192377]
19. Lai WM, Hou JS, Mow VC. 1991 A triphasic theory for the swelling and deformation behaviors of articular cartilage. J. Biomech. Eng. 113:245–58 [PubMed: 1921350]
20. Maroudas A, Muir H, Wingham J. 1969 The correlation of fixed negative charge with glycosaminoglycan content of human articular cartilage. Biochim. Biophys. Acta 177:492–500 [PubMed: 4239606]
21. Minns RJ, Steven FS. 1977 The collagen fibril organization in human articular cartilage. J. Anat. 123(Part 2):437–57 [PubMed: 870478]
22. Jay GD. 2009 Characterization of a bovine synovial fluid lubricating factor. I. Chemical, surface activity and lubricating properties. Connect. Tissue Res. 28:71–88
23. Jones ARC, Gleghorn JP, Hughes CE, Fitz LJ, Zollner R, et al. 2007 Binding and localization of recombinant lubricin to articular cartilage surfaces. J. Orthop. Res. 25:283–92 [PubMed: 17106881]
24. Bonnevie ED, Galesso D, Secchieri C, Cohen I, Bonassar LJ. 2015 Elastoviscous transitions of articular cartilage reveal a mechanism of synergy between lubricin and hyaluronic acid. PLOS ONE 10:e0143415 [PubMed: 26599797]
25. Schinagl RM, Gurskis D, Chen AC, Sah RL. 1997 Depth-dependent confined compression modulus of full-thickness bovine articular cartilage. J. Orthop. Res. 15:499–506 [PubMed: 9379258]
26. Buckley MR, Bergou AJ, Fouchard J, Bonassar LJ, Cohen I. 2010 High-resolution spatial mapping of shear properties in cartilage. J. Biomech. 43:796–800 [PubMed: 19896130]
27. Charlebois M, McKee MD, Buschmann MD. 2004 Nonlinear tensile properties of bovine articular cartilage and their variation with age and depth. J. Biomech. Eng. 126:129–37 [PubMed: 15179842]
28. Buckley MR, Bonassar LJ, Cohen I. 2013 Localization of viscous behavior and shear energy dissipation in articular cartilage under dynamic shear loading. J. Biomech. Eng. 135:031002
29. Bartell LR, Fortier LA, Bonassar LJ, Cohen I. 2015 Measuring microscale strain fields in articular cartilage during rapid impact reveals thresholds for chondrocyte death and a protective role for the superficial layer. J. Biomech. 48:3440–46 [PubMed: 26150096]
30. Pearle AD, Warren RF, Rodeo SA. 2005 Basic science of articular cartilage and osteoarthritis. Clin. Sports Med. 24:1–12 [PubMed: 15636773]
31. Bi X, Yang X, Bostrom MPG, Bartusik D, Ramaswamy S, et al. 2007 Fourier transform infrared imaging and MR microscopy studies detect compositional and structural changes in cartilage in a rabbit model of osteoarthritis. Anal. Bioanal. Chem. 387:1601–12 [PubMed: 17143596]
32. Boskey A, Pleshko Camacho N. 2007 FT-IR imaging of native and tissue-engineered bone and cartilage. Biomaterials 28:2465–78 [PubMed: 17175021]
33. Bae WC, Temple MM, Amiel D, Coutts RD, Niederauer GG, Sah RL. 2003 Indentation testing of human cartilage: sensitivity to articular surface degeneration. Arthritis Rheum. 48:3382–94 [PubMed: 14673990]
34. Oettmeier R, Abendroth K. 1989 Osteoarthritis and bone: osteologic types of osteoarthritis of the hip. Skelet. Radiol. 18:165–74

35. Vacanti JP, Langer R. 1999 Tissue engineering: the design and fabrication of living replacement devices for surgical reconstruction and transplantation. Lancet 354:S32–34
36. Dimicco MA, Sah RL. 2001 Integrative cartilage repair: Adhesive strength is correlated with collagen deposition. J. Orthop. Res. 19:1105–12 [PubMed: 11781012]
37. Klein TJ, Schumacher BL, Schmidt TA, Li KW, Voegtline MS, et al. 2003 Tissue engineering of stratified articular cartilage from chondrocyte subpopulations. Osteoarthr. Cartil. 11:595–602
38. Kim M, Farrell MJ, Steinberg DR, Burdick JA, Mauck RL. 2017 Enhanced nutrient transport improves the depth-dependent properties of tri-layered engineered cartilage constructs with zonal co-culture of chondrocytes and MSCs. Acta Biomater. 58:1–11 [PubMed: 28629894]
39. Kim T-K, Sharma B, Williams C, Ruffner M, Malik A, et al. 2003 Experimental model for cartilage tissue engineering to regenerate the zonal organization of articular cartilage. Osteoarthr. Cartil. 11:653–64
40. Sharma B, Williams CG, Kim TK, Sun D, Malik A, et al. 2007 Designing zonal organization into tissue-engineered cartilage. Tissue Eng. 13:405–14 [PubMed: 17504064]
41. Ng KW, Ateshian GA, Hung CT. 2009 Zonal chondrocytes seeded in a layered agarose hydrogel create engineered cartilage with depth-dependent cellular and mechanical inhomogeneity. Tissue Eng. A 15:2315–24
42. Benya PD, Padilla SR, Nimni ME. 1978 Independent regulation of collagen types by chondrocytes during the loss of differentiated function in culture. Cell 15:1313–21 [PubMed: 729001]
43. Darling EM, Athanasiou KA. 2005 Rapid phenotypic changes in passaged articular chondrocyte subpopulations. J. Orthop. Res. 23:425–32 [PubMed: 15734258]
44. Li W-J, Tuli R, Okafor C, Derfoul A, Danielson KG, et al. 2005 A three-dimensional nanofibrous scaffold for cartilage tissue engineering using human mesenchymal stem cells. Biomaterials 26:599–609 [PubMed: 15282138]
45. Caplan AI. 2007 Adult mesenchymal stem cells for tissue engineering versus regenerative medicine. J. Cell. Physiol. 213:341–47 [PubMed: 17620285]
46. Alhadlaq A, Elisseeff JH, Hong L, Williams CG, Caplan AI, et al. 2004 Adult stem cell driven genesis of human-shaped articular condyle. Ann. Biomed. Eng. 32:911–23 [PubMed: 15298429]
47. Vinardell T, Sheehy EJ, Buckley CT, Kelly DJ. 2012 A comparison of the functionality and in vivo phenotypic stability of cartilaginous tissues engineered from different stem cell sources. Tissue Eng. A 18:1161–70
48. Pelttari K, Winter A, Steck E, Goetzke K, Hennig T, et al. 2006 Premature induction of hypertrophy during in vitro chondrogenesis of human mesenchymal stem cells correlates with calcification and vascular invasion after ectopic transplantation in SCID mice. Arthritis Rheum. 54:3254–66 [PubMed: 17009260]
49. Chawla K, Klein TJ, Schumacher BL, Jadin KD, Shah BH, et al. 2007 Short-term retention of labelled chondrocyte subpopulations in stratified tissue-engineered cartilaginous constructs implanted in vivo in mini-pigs. Tissue Eng. 13:1525–37 [PubMed: 17532744]
50. Schaefer D, Martin I, Shastri P, Padera R, Langer R, et al. 2000 In vitro generation of osteochondral composites. Biomaterials 21:2599–606 [PubMed: 11071609]
51. Steinmetz NJ, Aisenbrey EA, Westbrook KK, Qi HJ, Bryant SJ. 2015 Mechanical loading regulates human MSC differentiation in a multi-layer hydrogel for osteochondral tissue engineering. Acta Biomater. 21:142–53 [PubMed: 25900444]
52. Sherwood JK, Riley SL, Palazzolo R, Brown SC, Monkhouse DC, et al. 2002 A three-dimensional osteochondral composite scaffold for articular cartilage repair. Biomaterials 23:4739–51 [PubMed: 12361612]
53. Ahn J-H, Lee T-H, Oh J-S, Kim S-Y, Kim H-J, et al. 2009 A novel hyaluronate-atelocollagen/β-TCP-hydroxyapatite biphasic scaffold for the repair of osteochondral defects in rabbits. Tissue Eng. A 15:2595–604
54. Guo X, Park H, Young S, Kretlow JD, van den Beucken JJ, et al. 2010 Repair of osteochondral defects with biodegradable hydrogel composites encapsulating marrow mesenchymal stem cells in a rabbit model. Acta Biomater. 6:39–47 [PubMed: 19660580]
55. Cao Z, Hou S, Sun D, Wang X, Tang J. 2012 Osteochondral regeneration by a bilayered construct in a cell-free or cell-based approach. Biotechnol. Lett. 34:1151–57 [PubMed: 22361963]

56. Chen J, Chen H, Li P, Diao H, Zhu S, et al. 2011 Simultaneous regeneration of articular cartilage and subchondral bone in vivo using MSCs induced by a spatially controlled gene delivery system in bilayered integrated scaffolds. Biomaterials 32:4793–805 [PubMed: 21489619]
57. Cui W, Wang Q, Chen G, Zhou S, Chang Q, et al. 2011 Repair of articular cartilage defects with tissue-engineered osteochondral composites in pigs. J. Biosci. Bioeng. 111:493–500 [PubMed: 21208828]
58. Griffin DJ, Bonnevie ED, Lachowsky DJ, Hart JCA, Sparks HD, et al. 2015 Mechanical characterization of matrix-induced autologous chondrocyte implantation (MACI®) grafts in an equinemodelat53weeks. J. Biomech. 48:1944–49 [PubMed: 25920896]
59. Wang X, Wenk E, Zhang X, Meinel L, Vunjak-Novakovic G, Kaplan DL. 2009 Growth factor gradients via microsphere delivery in biopolymer scaffolds for osteochondral tissue engineering. J. Control. Release 134:81–90 [PubMed: 19071168]
60. Mohan N, Dormer NH, Caldwell KL, Key VH, Berkland CJ, Detamore MS. 2011 Continuous gradients of material composition and growth factors for effective regeneration of the osteochondral interface. Tissue Eng. A 17:2845–55
61. Grayson WL, Bhumiratana S, Chao PHG, Hung CT, Vunjak-Novakovic G. 2010 Spatial regulation of human mesenchymal stem cell differentiation in engineered osteochondral constructs: effects of pre-differentiation, soluble factors and medium perfusion. Osteoarthr. Cartil. 18:714–23
62. Lu S, Lam J, Trachtenberg JE, Lee EJ, Seyednejad H, et al. 2014 Dual growth factor delivery from bi-layered, biodegradable hydrogel composites for spatially-guided osteochondral tissue repair. Biomaterials 35:8829–39 [PubMed: 25047629]
63. Alexander PG, Gottardi R, Lin H, Lozito TP, Tuan RS. 2014 Three-dimensional osteogenic and chondrogenic systems to model osteochondral physiology and degenerative joint diseases. Exp. Biol. Med. 239:1080–95
64. Chen SS, Falcovitz YH, Schneiderman R, Maroudas A, Sah RL. 2001 Depth-dependent compressive properties of normal aged human femoral head articular cartilage: relationship to fixed charge density. Osteoarthr. Cartil. 9:561–69
65. Kelly T-AN, Ng KW, Wang CC-B, Ateshian GA, Hung CT. 2006 Spatial and temporal development of chondrocyte-seeded agarose constructs in free-swelling and dynamically loaded cultures. J. Biomech. 39:1489–97 [PubMed: 15990101]
66. Farrell MJ, Comeau ES, Mauck RL. 2012 Mesenchymal stem cells produce functional cartilage matrix in three-dimensional culture in regions of optimal nutrient supply. Eur. Cell. Mater. 23:425–40 [PubMed: 22684531]
67. Campbell SE, Ferguson VL, Hurley DC. 2012 Nanomechanical mapping of the osteochondral interface with contact resonance force microscopy and nanoindentation. Acta Biomater. 8:4389–96 [PubMed: 22877818]
68. Stolz M, Gottardi R, Raiteri R, Miot S, Martin I, et al. 2009 Early detection of aging cartilage and osteoarthritis in mice and patient samples using atomic force microscopy. Nat. Nanotechnol. 4:186–92 [PubMed: 19265849]
69. Kim M, Bi X, Horton WE, Spencer RG, Pleshko Camacho N. 2005 Fourier transform infrared imaging spectroscopic analysis of tissue engineered cartilage: histologic and biochemical correlations. J. Biomed. Opt. 10:031105 [PubMed: 16229630]
70. Pleshko Camacho N, West P, Torzilli PA, Mendelsohn R. 2001 FTIR microscopic imaging of collagen and proteoglycan in bovine cartilage. Biopolymers 62:1–8 [PubMed: 11135186]
71. Bonifacio A, Beleites C, Vittur F, Marsich E, Semeraro S, et al. 2010 Chemical imaging of articular cartilage sections with Raman mapping, employing uni- and multi-variate methods for data analysis. Analyst 135:3193–204 [PubMed: 20967391]
72. Bergholt MS, St-Pierre J-P, Offeddu GS, Parmar PA, Albro MB, et al. Raman spectroscopy reveals new insights into the zonal organization of native and tissue-engineered articular cartilage. ACS Cent. Sci. 2:885–95 [PubMed: 28058277]
73. Griffin DJ, Ortved KF, Nixon AJ, Bonassar LJ. 2016 Mechanical properties and structure–function relationships in articular cartilage repaired using IGF-I gene–enhanced chondrocytes. J. Orthop. Res. 34:149–53 [PubMed: 26308948]

74. Thomopoulos S, Marquez JP, Weinberger B, Birman V, Genin GM. 2006 Collagen fiber orientation at the tendon to bone insertion and its influence on stress concentrations. J. Biomech. 39:1842–51 [PubMed: 16024026]
75. Genin GM, Kent A, Birman V, Wopenka B, Pasteris JD, et al. 2009 Functional grading of mineral and collagen in the attachment of tendon to bone. Biophys. J. 97:976–85 [PubMed: 19686644]
76. Rossetti L, Kuntz LA, Kunold E, Schock J, Müller KW, et al. 2017 The microstructure and micromechanics of the tendon–bone insertion. Nat. Mater. 16:664–70 [PubMed: 28250445]
77. Spalazzi JP, Boskey AL, Pleshko N, Lu HH, Kepler C. 2013 Quantitative mapping of matrix content and distribution across the ligament-to-bone insertion. PLOS ONE 8:e74349 [PubMed: 24019964]
78. Hyman J, Rodeo SA. 2000 Injury and repair of tendons and ligaments. Phys. Med. Rehabil. Clin. N. Am. 11:267–88 [PubMed: 10810761]
79. Woo SL-Y, Debski RE, Zeminski J, Abramowitch SD, Saw SS, Fenwick JA. 2000 Injury and repair of ligaments and tendons. Annu. Rev. Biomed. Eng. 2:83–118 [PubMed: 11701508]
80. Lin TW, Cardenas L, Soslowsky LJ. 2004 Biomechanics of tendon injury and repair. J. Biomech. 37:865–77 [PubMed: 15111074]
81. Gomez M 1995 The physiology and biochemistry of soft tissue healing In Rehabilitation of the Injured Knee, ed. Griffin L, pp. 34–44. St. Louis, MO: Mosby
82. Rodeo SA, Arnoczky SP, Torzilli PA, Hidaka C, Warren RF. 1993 Tendon-healing in a bone tunnel. A biomechanical and histological study in the dog. J. Bone Jt. Surg. Am. 75:1795–803
83. Dyment NA, Breidenbach AP, Schwartz AG, Russell RP, Aschbacher-Smith L, et al. 2015 *Gdf5* progenitors give rise to fibrocartilage cells that mineralize via hedgehog signaling to form the zonal enthesis. Dev. Biol. 405:96–107 [PubMed: 26141957]
84. Schwartz AG, Long F, Thomopoulos S. 2014 Enthesis fibrocartilage cells originate from a population of Hedgehog-responsive cells modulated by the loading environment. Development 142:196–206
85. Killian ML, Thomopoulos S. 2016 Scleraxis is required for the development of a functional tendon enthesis. FASEB J. 30:301–11 [PubMed: 26443819]
86. Smith L, Xia Y, Galatz LM, Genin GM, Thomopoulos S. 2012 Tissue-engineering strategies for the tendon/ligament-to-bone insertion. Connect. Tissue Res. 53:95–105 [PubMed: 22185608]
87. Lu HH, Thomopoulos S. 2013 Functional attachment of soft tissues to bone: development, healing, and tissue engineering. Annu. Rev. Biomed. Eng. 15:201–26 [PubMed: 23642244]
88. Kryger GS, Chong AKS, Costa M, Pham H, Bates SJ, Chang J. 2007 A comparison of tenocytes and mesenchymal stem cells for use in flexor tendon tissue engineering. J. Hand Surg. Am. 32:597–605 [PubMed: 17481995]
89. Chen X, Yin Z, Chen J, Liu H, Shen W, et al. 2014 *Scleraxis*-overexpressed human embryonic stem cell–derived mesenchymal stem cells for tendon tissue engineering with knitted silk-collagen scaffold. Tissue Eng. A 20:1583–92
90. Pham QP, Sharma U, Mikos AG. 2006 Electrospinning of polymeric nanofibers for tissue engineering applications: a review. Tissue Eng. 12:1197–211 [PubMed: 16771634]
91. Li W-J, Mauck RL, Cooper JA, Yuan X, Tuan RS. 2007 Engineering controllable anisotropy in electrospun biodegradable nanofibrous scaffolds for musculoskeletal tissue engineering. J. Biomech. 40:1686–93 [PubMed: 17056048]
92. Shin HJ, Lee CH, Cho IH, Kim Y-J, Lee Y-J, et al. 2006 Electrospun PLGA nanofiber scaffolds for articular cartilage reconstruction: mechanical stability, degradation and cellular responses under mechanical stimulation in vitro. J. Biomater. Sci. Polym. Ed. 17:103–19 [PubMed: 16411602]
93. Li W-J, Cooper JA, Mauck RL, Tuan RS. 2006 Fabrication and characterization of six electrospun poly (α-hydroxy ester)-based fibrous scaffolds for tissue engineering applications. Acta Biomater. 2:377–85 [PubMed: 16765878]
94. Zhang X, Reagan MR, Kaplan DL. 2009 Electrospun silk biomaterial scaffolds for regenerative medicine. Adv. Drug Deliv. Rev. 61:988–1006 [PubMed: 19643154]
95. Huang Z-M, Zhang Y, Ramakrishna S, Lim C. 2004 Electrospinning and mechanical characterization of gelatin nanofibers. Polymer 45:5361–68

96. Kim IL, Mauck RL, Burdick JA. 2011 Hydrogel design for cartilage tissue engineering: a case study with hyaluronic acid. Biomaterials 32:8771–82 [PubMed: 21903262]

97. Matthews JA, Wnek GE, Simpson DG, Bowlin GL. 2002 Electrospinning of collagen nanofibers. Biomacromolecules 3:232–38 [PubMed: 11888306]

98. Choi JS, Lee SJ, Christ GJ, Atala A, Yoo JJ. 2008 The influence of electrospun aligned poly(ε-caprolactone)/collagen nanofiber meshes on the formation of self-aligned skeletal muscle myotubes. Biomaterials 29:2899–906 [PubMed: 18400295]

99. Awad HA, Butler DL, Harris MT, Ibrahim RE, Wu Y, et al. 2000 In vitro characterization of mesenchymal stem cell–seeded collagen scaffolds for tendon repair: effects of initial seeding density on contraction kinetics. J. Biomed. Mater. Res. 51:233–40 [PubMed: 10825223]

100. Barocas VH, Tranquillo RT. 1997 An anisotropic biphasic theory of tissue-equivalent mechanics: the interplay among cell traction, fibrillar network deformation, fibril alignment, and cell contact guidance. J. Biomech. Eng. 119:137–45 [PubMed: 9168388]

101. Puetzer JL, Koo E, Bonassar LJ. 2015 Induction of fiber alignment and mechanical anisotropy in tissue engineered menisci with mechanical anchoring. J. Biomech. 48:1436–43 [PubMed: 25770753]

102. Sander EA, Stylianopoulos T, Tranquillo RT, Barocas VH. 2009 Image-based multiscale modelling predicts tissue-level and network-level fiber reorganization in stretched cell-compacted collagen gels. PNAS 106:17675–80 [PubMed: 19805118]

103. Li X, Xie J, Lipner J, Yuan X, Thomopoulos S, Xia Y. 2009 Nanofiber scaffolds with gradations in mineral content for mimicking the tendon-to-bone insertion site. Nano Lett. 9:2763–68 [PubMed: 19537737]

104. Erisken C, Kalyon DM, Wang H. 2008 Functionally graded electrospun polycaprolactone and β-tricalcium phosphate nanocomposites for tissue engineering applications. Biomaterials 29:4065–73 [PubMed: 18649939]

105. Phillips JE, Burns KL, Le Doux JM, Guldberg RE, Garcia AJ. 2008 Engineering graded tissue interfaces. PNAS 105:12170–75 [PubMed: 18719120]

106. Smith LJ, Deymier AC, Boyle JJ, Li Z, Linderman SW, et al. 2016 Tunability of collagen matrix mechanical properties via multiple modes of mineralization. Interface Focus 6:20150070 [PubMed: 26855755]

107. Boyle JJ, Kume M, Wyczalkowski MA, Taber LA, Pless RB, et al. 2014 Simple and accurate methods for quantifying deformation, disruption, and development in biological tissues. J. R. Soc. Interface 11:20140685 [PubMed: 25165601]

108. Furseth Klinge R 2001 The structure of the fibrous tissue on the articular surface of the temporal bone in the monkey *(Macaca mulatta)*. Micron 32:551–57 [PubMed: 11166575]

109. Furseth Klinge R 1996 The structure of the mandibular condyle in the monkey *(Macaca mulatta)*. Micron 27:381–87 [PubMed: 9008876]

110. Delatte M, Von den Hoff JW, van Rheden REM, Kuijpers-Jagtman AM. 2004 Primary and secondary cartilages of the neonatal rat: the femoral head and the mandibular condyle. Eur. J. Oral Sci. 112:156–62 [PubMed: 15056113]

111. Dormer NH, Busaidy K, Berkland CJ, Detamore MS. 2011 Osteochondral interface regeneration of rabbit mandibular condyle with bioactive signal gradients. J. Oral Maxillofac. Surg. 69:e50–57 [PubMed: 21470747]

112. Hollister S, Lin C, Saito E, Lin C, Schek R, et al. 2005 Engineering craniofacial scaffolds. Orthod. Craniofac. Res. 8:162–73 [PubMed: 16022718]

113. Murphy MK, MacBarb RF, Wong ME, Athanasiou KA. 2013 Temporomandibular disorders: a review of etiology, clinical management, and tissue engineering strategies. Int. J. Oral Maxillofac. Implants 28:e393–414 [PubMed: 24278954]

114. Bailey MM, Wang L, Bode CJ, Mitchell KE, Detamore MS. 2007 A comparison of human umbilical cord matrix stem cells and temporomandibular joint condylar chondrocytes for tissue engineering temporomandibular joint condylar cartilage. Tissue Eng. 13:2003–10 [PubMed: 17518722]

115. Wang L, Detamore MS. 2007 Tissue engineering the mandibular condyle. Tissue Eng. 13:1955–71 [PubMed: 17518708]

116. Detamore MS, Athanasiou KA. 2003 Structure and function of the temporomandibular joint disc: Implications for tissue engineering. J. Oral Maxillofac. Surg. 61:494–506 [PubMed: 12684970]
117. Detamore MS, Athanasiou KA. 2003 Motivation, characterization, and strategy for tissue engineering the temporomandibular joint disc. Tissue Eng. 9:1065–87 [PubMed: 14670096]
118. Zimmerman BK, Bonnevie ED, Park M, Zhou Y, Wang L, et al. 2015 Role of interstitial fluid pressurization in TMJ lubrication. J. Dent. Res. 94:85–92 [PubMed: 25297115]
119. Bonnevie ED, Baro V, Wang L, Burris DL. 2011 In-situ studies of cartilage microtribology: roles ofspeed and contact area. Tribol. Lett. 41:83–95 [PubMed: 21765622]
120. Ateshian GA.2009TheroleofinterstitialfluidpressurizationinarticularcartilagelubricationJ.Biomech. 42:1163–76 [PubMed: 19464689]
121. Bonnevie ED, Baro VJ, Wang L, Burris DL. 2012 Fluid load support during localized indentation of cartilage with a spherical probe. J. Biomech. 45:1036–41 [PubMed: 22284430]
122. Weng Y, Cao Y, Arevalo C, Vacanti MP, Vacanti CA. 2001 Tissue-engineered composites of bone and cartilage for mandible condylar reconstruction. J. Oral Maxillofac. Surg. 59:185–90 [PubMed: 11213987]
123. Schek R, Taboas J, Hollister S, Krebsbach P. 2005 Tissue engineering osteochondral implants for temporomandibular joint repair. Orthod. Craniofac. Res. 8:313–19 [PubMed: 16238612]
124. Alhadlaq A, Mao JJ. 2003 Tissue-engineered neogenesis of human-shaped mandibular condyle from rat mesenchymal stem cells. J. Dent. Res. 82:951–56 [PubMed: 14630893]
125. Feinberg SE, Hollister SJ, Halloran JW, Chu TM, Krebsbach PH. 2001 Image-based biomimetic approach to reconstruction of the temporomandibular joint. Cells Tissues Organs 169:309–21 [PubMed: 11455128]
126. Johannessen W, Elliott DM. 2005 Effects of degeneration on the biphasic material properties of human nucleus pulposus in confined compression. Spine 30:E724–29 [PubMed: 16371889]
127. Urban JP, McMullin JF. 1988 Swelling pressure of the lumbar intervertebral discs: influence of age, spinal level, composition, and degeneration. Spine 13:179–87 [PubMed: 3406838]
128. Cassidy JJ, Hiltner A, Baer E. 1989 Hierarchical structure of the intervertebral disc. Connect. Tissue Res. 23:75–88 [PubMed: 2632144]
129. Moon SM, Yoder JH, Wright AC, Smith LJ, Vresilovic EJ, Elliott DM. 2013 Evaluation of intervertebral disc cartilaginous endplate structure using magnetic resonance imaging. Eur. Spine J. 22:1820–28 [PubMed: 23674162]
130. Gullbrand SE, Ashinsky BG, Martin JT, Pickup S, Smith LJ, et al. 2016 Correlations between quantitative $T2$ and $T1\rho$ MRI, mechanical properties and biochemical composition in a rabbit lumbar intervertebral disc degeneration model. J. Orthop. Res. 34:1382–88 [PubMed: 27105019]
131. Luoma K, Riihimäki H, Luukkonen R, Raininko R, Viikari-Juntura E, Lamminen A. 2000 Low back pain in relation to lumbar disc degeneration. Spine 25:487–92 [PubMed: 10707396]
132. Bhattacharjee M, Miot S, Gorecka A, Singha K, Loparic M, et al. 2012 Oriented lamellar silk fibrous scaffolds to drive cartilage matrix orientation: towards annulus fibrosus tissue engineering. Acta Biomater. 8:3313–25 [PubMed: 22641105]
133. Wan Y, Feng G, Shen FH, Laurencin CT, Li X. 2008 Biphasic scaffold for annulus fibrosus tissue regeneration. Biomaterials 29:643–52 [PubMed: 17997480]
134. Sato M, Asazuma T, Ishihara M, Ishihara M, Kikuchi T, et al. 2003 An experimental study of the regeneration of the intervertebral disc with an allograft of cultured annulus fibrosus cells using a tissue-engineering method. Spine 28:548–53 [PubMed: 12642760]
135. Moriguchi Y, Borde B, Grunert P, Khair T, Hudson K, et al. 2015 Annular repair using high-density collagen gels seeded with fibrochondrocytes: in vivo outcome in the rodent spine. Spine J. 15:S187–88
136. Nerurkar NL, Elliott DM, Mauck RL. 2007 Mechanics of oriented electrospun nanofibrous scaffolds for annulus fibrosus tissue engineering. J. Orthop. Res. 25:1018–28 [PubMed: 17457824]
137. Nerurkar NL, Baker BM, Sen S, Wible EE, Elliott DM, Mauck RL. 2009 Nanofibrous biologic laminates replicate the form and function of the annulus fibrosus. Nat. Mater. 8:986–92 [PubMed: 19855383]

138. Moriguchi Y, Mojica-Santiago J, Grunert P, Pennicooke B, Berlin C, et al. 2017 Total disc replacement using tissue-engineered intervertebral discs in the canine cervical spine. PLOS ONE 12:e0185716 [PubMed: 29053719]
139. Mwale F, Roughley P, Antoniou J. 2004 Distinction between the extracellular matrix of the nucleus pulposus and hyaline cartilage: a requisite for tissue engineering of intervertebral disc. Eur. Cell. Mater. 8:58–63 [PubMed: 15602703]
140. Iatridis JC, Setton LA, Weidenbaum M, Mow VC. 1997 The viscoelastic behaviour of the non-degenerate human lumbar nucleus pulposus in shear. J. Biomech. 30:1005–13 [PubMed: 9391867]
141. Séguin CA, Grynpas MD, Pilliar RM, Waldman SD, Kandel RA. 2004 Tissue engineered nucleuś pulposus tissue formed on a porous calcium polyphosphate substrate. Spine 29:1299–306 [PubMed: 15187628]
142. Chou AI, Akintoye SO, Nicoll SB. 2009 Photo-crosslinked alginate hydrogels support enhanced matrix accumulation by nucleus pulposus cells in vivo. Osteoarthr. Cartil. 17:1377–84
143. Roughley P, Hoemann C, DesRosiers E, Mwale F, Antoniou J, Alini M. 2006 The potential of chitosan-based gels containing intervertebral disc cells for nucleus pulposus supplementation. Biomaterials 27:388–96 [PubMed: 16125220]
144. Risbud MV, Albert TJ, Guttapalli A, Vresilovic EJ, Hillibrand AS, et al. 2004 Differentiation of mesenchymal stem cells towards a nucleus pulposus–like phenotype in vitro: implications for cell-based transplantation therapy. Spine 29:2627–32 [PubMed: 15564911]
145. Hunter CJ, Matyas JR, Duncan NA. 2003 The notochordal cell in the nucleus pulposus: a review in the context of tissue engineering. Tissue Eng. 9:667–77 [PubMed: 13678445]
146. Lee K-I, Moon S-H, Kim H, Kwon U-H, Kim H-J, et al. 2012 Tissue engineering of the intervertebral disc with cultured nucleus pulposus cells using atelocollagen scaffold and growth factors. Spine 37:452–58 [PubMed: 22037529]
147. Stoyanov JV, Gantenbein-Ritter B, Bertolo A, Aebli N, Baur M, et al. 2011 Role of hypoxia and growth and differentiation factor 5 on differentiation of human mesenchymal stem cells towards intervertebral nucleus pulposus–like cells. Eur. Cell. Mater. 21:533–47 [PubMed: 21710444]
148. Mizuno H, Roy AK, Zaporojan V, Vacanti CA, Ueda M, Bonassar LJ. 2006 Biomechanical and biochemical characterization of composite tissue-engineered intervertebral discs. Biomaterials 27:362–70 [PubMed: 16165204]
149. Mizuno H, Roy AK, Vacanti CA, Kojima K, Ueda M, Bonassar LJ. 2004 Tissue-engineered composites of anulus fibrosus and nucleus pulposus for intervertebral disc replacement. Spine 29:1290–87 [PubMed: 15187626]
150. Nerurkar NL, Sen S, Huang AH, Elliott DM, Mauck RL. 2010 Engineered disc-like angle-ply structures for intervertebral disc replacement. Spine 35:867–73 [PubMed: 20354467]
151. Nesti LJ, Li W-J, Shanti RM, Jiang YJ, Jackson W, et al. 2008 Intervertebral disc tissue engineeringusing a novel hyaluronic acid–nanofibrous scaffold (HANFS) amalgam. Tissue Eng. A 14:1527–37
152. Bowles RD, Williams RM, Zipfel WR, Bonassar LJ. 2010 Self-assembly of aligned tissue-engineered annulus fibrosus and intervertebral disc composite via collagen gel contraction. Tissue Eng. A 16:1339–48
153. Bowles RD, Gebhard HH, Hartl R, Bonassar LJ. 2011 Tissue-engineered intervertebral discs produce new matrix, maintain disc height, and restore biomechanical function to the rodent spine. PNAS 108:13106–11 [PubMed: 21808048]
154. Martin JT, Kim DH, Milby AH, Pfeifer CG, Smith LJ, et al. 2017 In vivo performance of an acellular disc-like angle ply structure (DAPS) for total disc replacement in a small animal model. J. Orthop. Res. 35:23–31 [PubMed: 27227357]
155. Martin JT, Milby AH, Chiaro JA, Kim DH, Hebela NM, et al. 2014 Translation of an engineered nanofibrous disc-like angle-ply structure for intervertebral disc replacement in a small animal model. Acta Biomater. 10:2473–81 [PubMed: 24560621]
156. Benneker LM, Heini PF, Alini M, Anderson SE, Ito K. 2005 2004 Young Investigator Award Winner: Vertebral endplate marrow contact channel occlusions and intervertebral disc degeneration. Spine 30:167–73 [PubMed: 15644751]

157. Martin JT, Gullbrand SE, Kim DH, Ikuta K, Pfeifer CG, et al. 2017 In vitro maturation and in vivo integration and function of an engineered cell-seeded disc-like angle ply structure (DAPS) for total disc arthroplasty. Sci. Rep. 7:15765 [PubMed: 29150639]

158. Engler AJ, Sen S, Sweeney HL, Discher DE. 2006 Matrix elasticity directs stem cell lineage specification. Cell 126:677–89 [PubMed: 16923388]

159. Han WM, Heo SJ, Driscoll TP, Delucca JF, McLeod CM, et al. 2016 Microstructural heterogeneity directs micromechanics and mechanobiology in native and engineered fibrocartilage. Nat. Mater.15:477–84 [PubMed: 26726994]

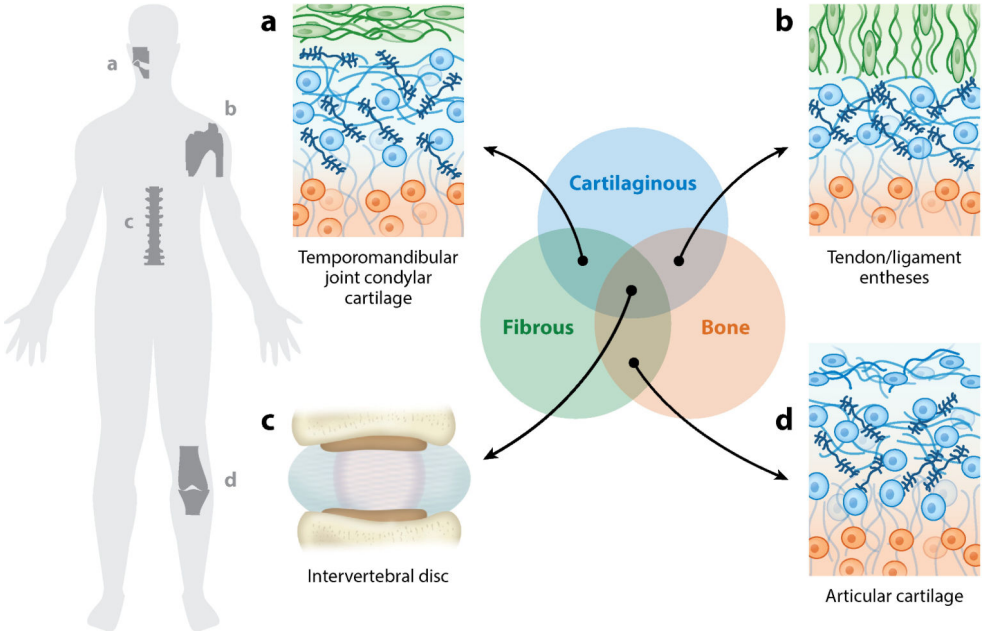

Figure 1.

Graded material connections are universal in the musculoskeletal system. In a simplified context, connective tissues can be grouped into cartilaginous (*blue*), fibrous (*green*), and calcified (i.e., bone) (*orange*) tissue types. The connections between these dissimilar materials are present throughout the body, and their mechanical importance and diversity pose obstacles for tissue engineering functional replacements. Examples include (*a*) the graded structure from the surface to the bone of the condylar cartilage in the temporomandibular joint; (*b*) the interface between tendon/ligament and bone; (*c*) the multiple interfaces among fibrous, cartilaginous, and bony tissue represented in the intervertebral disc of the spine; and (*d*) the interface between articular cartilage and bone (i.e., enthesis).

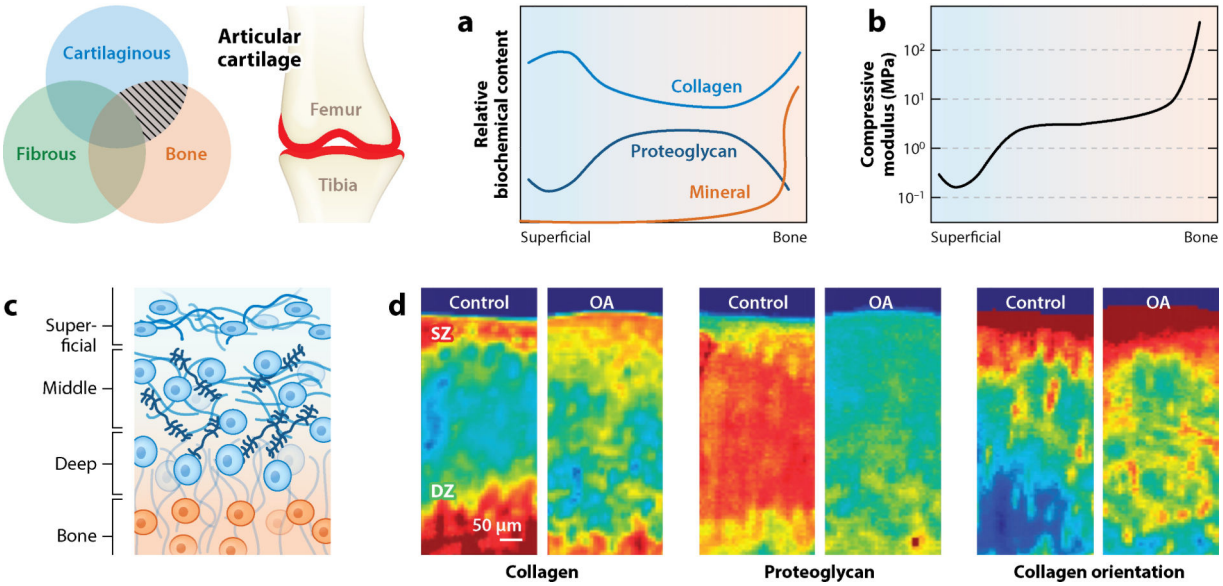

Figure 2.

Articular cartilage lines the ends of long bones (*highlighted in red*). This tissue exhibits a depth-dependent (*a*) biochemical and (*b*) mechanical profile—a compliant superficial zone transitions to stiffer and proteoglycan-rich middle and deep zones (2, 3, 26, 32). (*c*) Cellular, collagen (*blue*), and proteoglycan (*navy*) content evolves over the depth from the articular surface to subchondral bone (*orange*); between the deep zone and subchondral bone, stiffness increases rapidly in a mineralization-dependent manner (5). (*d*) Fourier transform infrared spectroscopic mapping of healthy and arthritic cartilage reveals that this depth-dependent profile is disrupted in disease and degeneration (colors indicate increasing content and organization from blue to red). Abbreviations: DZ, deep zone; OA, osteoarthritis; SZ, superficial zone. Panel *d* adapted with permission from Reference 32.

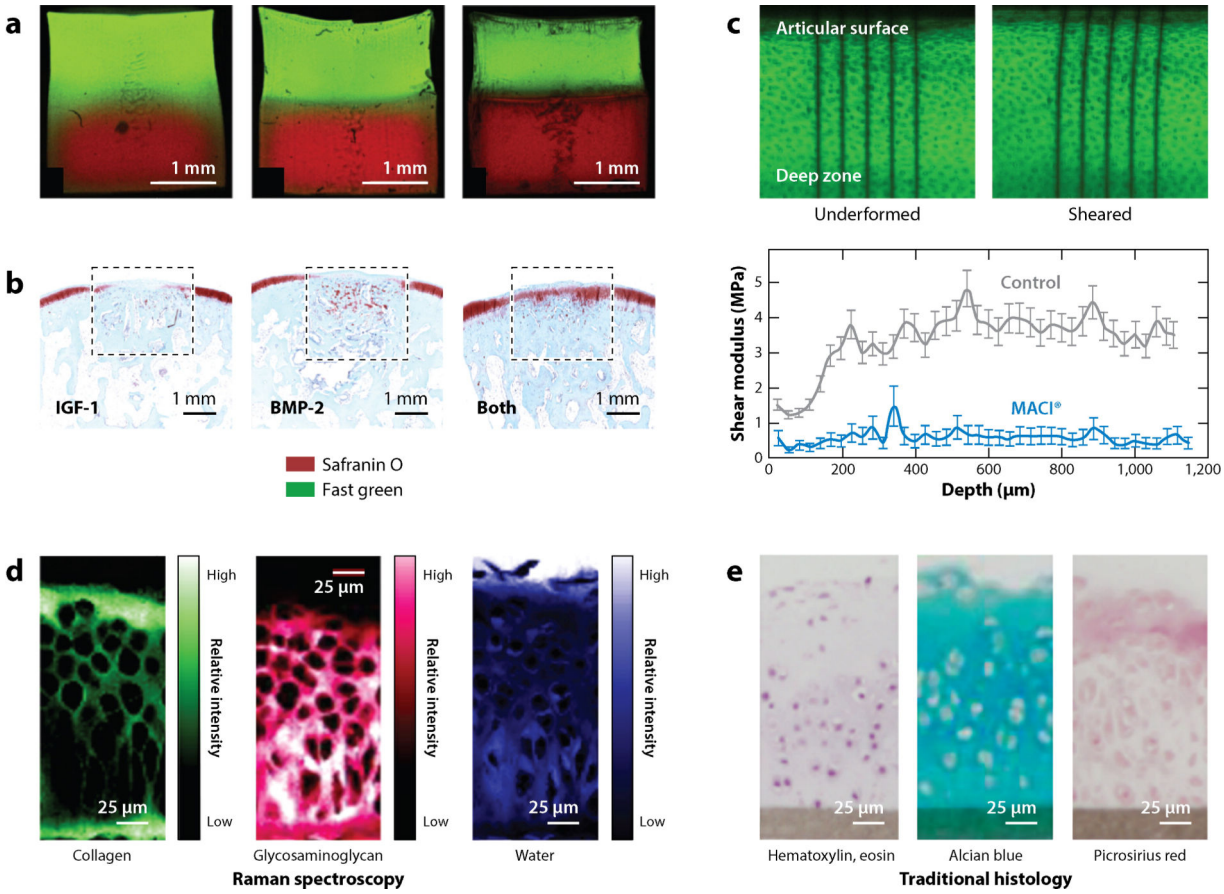

Figure 3.

Advances in generating and assessing graded cartilage structures. (*a*) Photocrosslinkable materials have emerged as a tool to generate material gradients. Steinmetz et al. (51) tuned polymerization times to demonstrate that a gradient between two materials can be controlled to produce (*left*) gradual to (*right*) abrupt material gradients. (*b*) Lu et al. (62) revealed that a composite material implant (*dashed boxes*) generated native-like tissue when coupled with cartilage- and bone-promoting growth factors (IGF-1 and BMP-2, respectively). (*c*) Griffin et al. (58) utilized elastography techniques to determine spatially varying mechanical properties of native and engineered tissue (26, 58). By analyzing the strain-mapped images of undeformed tissue before and after application of shear, the authors found that implanted cartilage (MACI®; *blue*) did not recapitulate native-like, graded properties (control; *gray*) even after 53 weeks of implantation. Spectroscopic techniques such as (*d*) Raman spectroscopy and (*e*) traditional histology enable quantitative analysis of the spatially varying biochemical content of native and engineered tissue. Abbreviations: BMP, bone morphogenetic protein; IGF, insulin-like growth factor. Panel *a* adapted from Reference 51 with permission. Panel *b* adapted from Reference 62 with permission. Panel *c* adapted from Reference 58 with permission. Panels *d* and *e* adapted from Reference 72 with permission; these are unofficial adaptations from an article that appeared in an ACS publication. ACS has not endorsed the content of these adaptations or the context of their use.

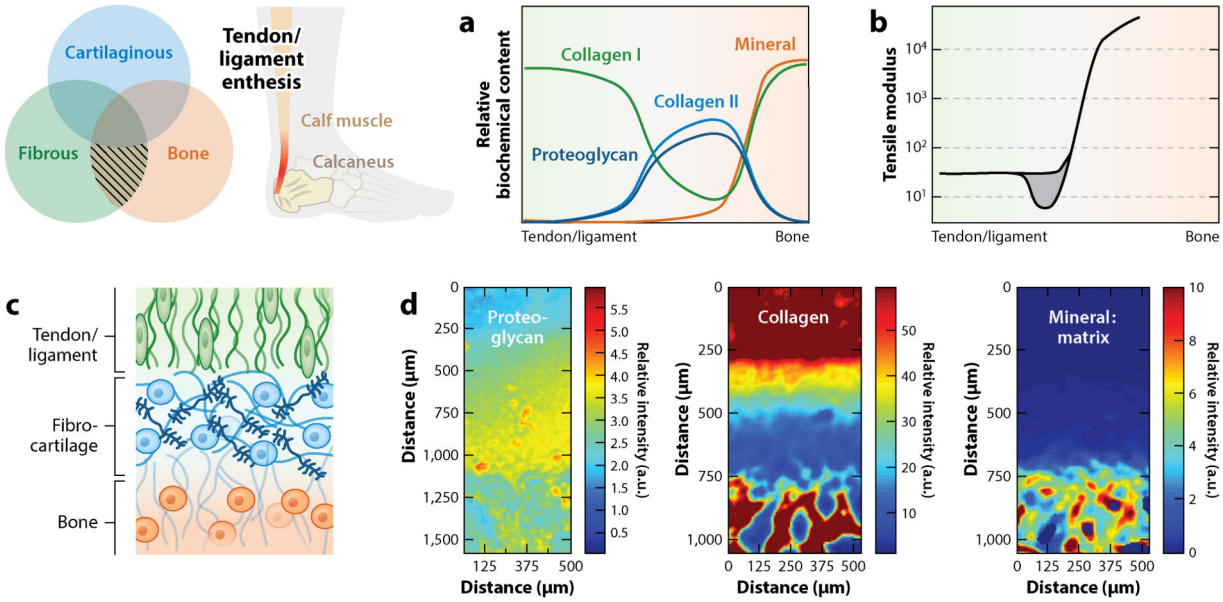

Figure 4.

Tendon and ligament entheses attach fibrous tissue to bone, e.g., the Achilles tendon (*highlighted in red*). These structures represent a complex interface with gradation in (*a*) extracellular matrix components that functionally correspond to (*b*) location-dependent mechanical properties. Of note is the inclusion of a compliant region (*gray*) between the fibrous tissue (*green*) and bone (*orange*) (8, 74). (*c*) This compliant inclusion is fibrocartilaginous in nature and exhibits spatially varying collagen makeup that shifts from type I (*green*) to type II (*blue*) collagen before transitioning to bone (*orange*). (*d*) Fourier transform infrared spectroscopic mapping of the enthesis reveals this spatial evolution of proteoglycans, collagen, and mineral content in the transition from fibrous tissue to bone. Abbreviation: a.u., arbitrary units. Panel *d* adapted from Reference 77 with permission.

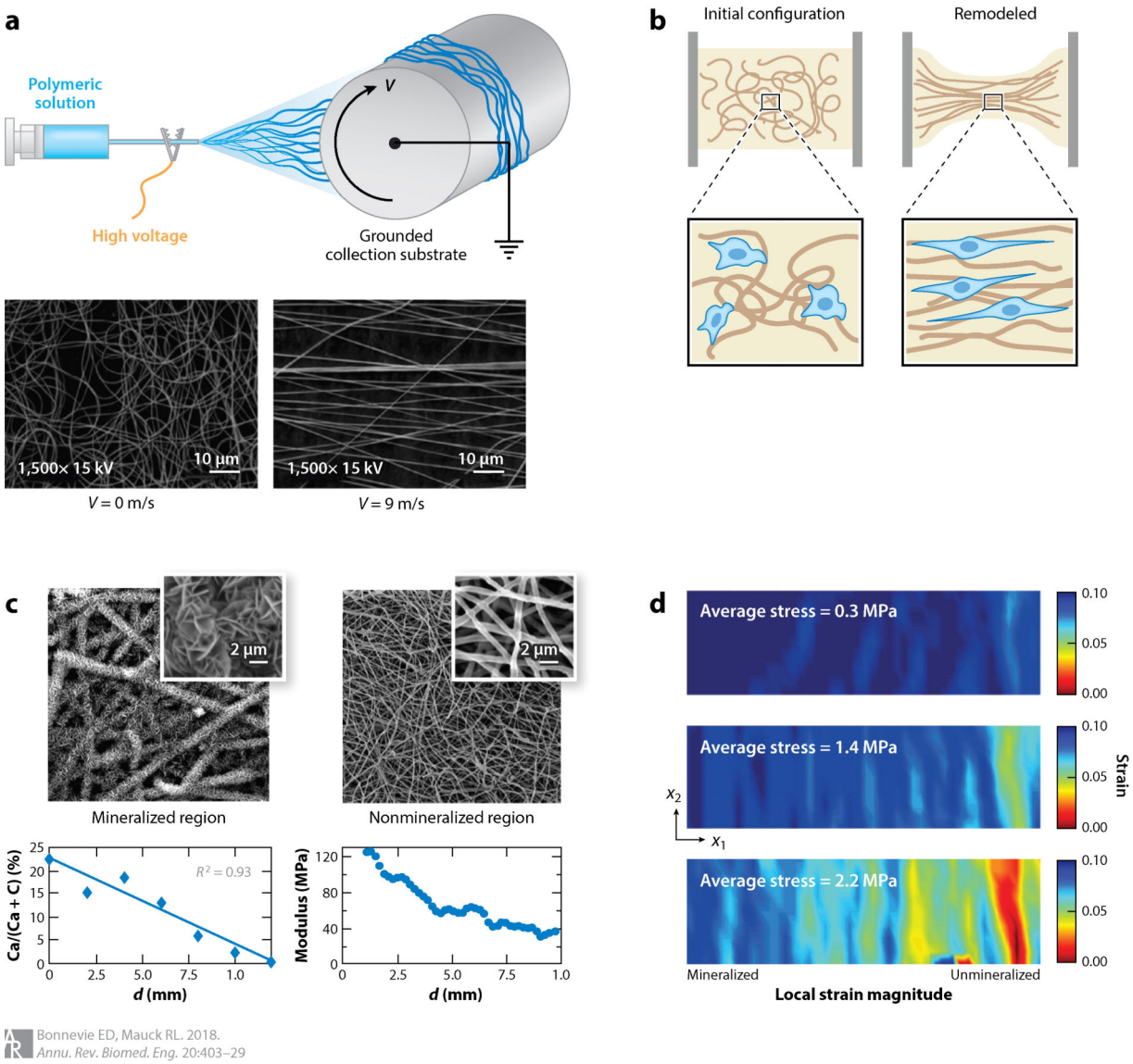

Figure 5.

(*a*) Electrospinning of synthetic polymeric materials, where a charged polymeric solution is collected onto a grounded substrate, is a promising technique to fabricate fibrous tissues with defined organization when deposited onto a spinning mandrel with surface velocity (*V*). (*b*) Aligned, fibrous materials can also be synthesized using natural materials such as collagen coupled with cell-based remodeling. Cell-mediated compaction of these gels has emerged as a powerful tool to instill organization into gels with predefined boundary conditions. (*c*,*d*) Mineralization of electrospun scaffolds can be used to mimic the graded material properties of the tendon enthesis. Li et al. (103) demonstrated that introducing a mineralization gradient within a scaffold (*c*) provides spatial gradation of mechanical properties, as revealed by strain mapping (*d*). Panel *a* adapted from Reference 91 with permission. Panels *c* and *d* adapted from Reference 103 with permission.

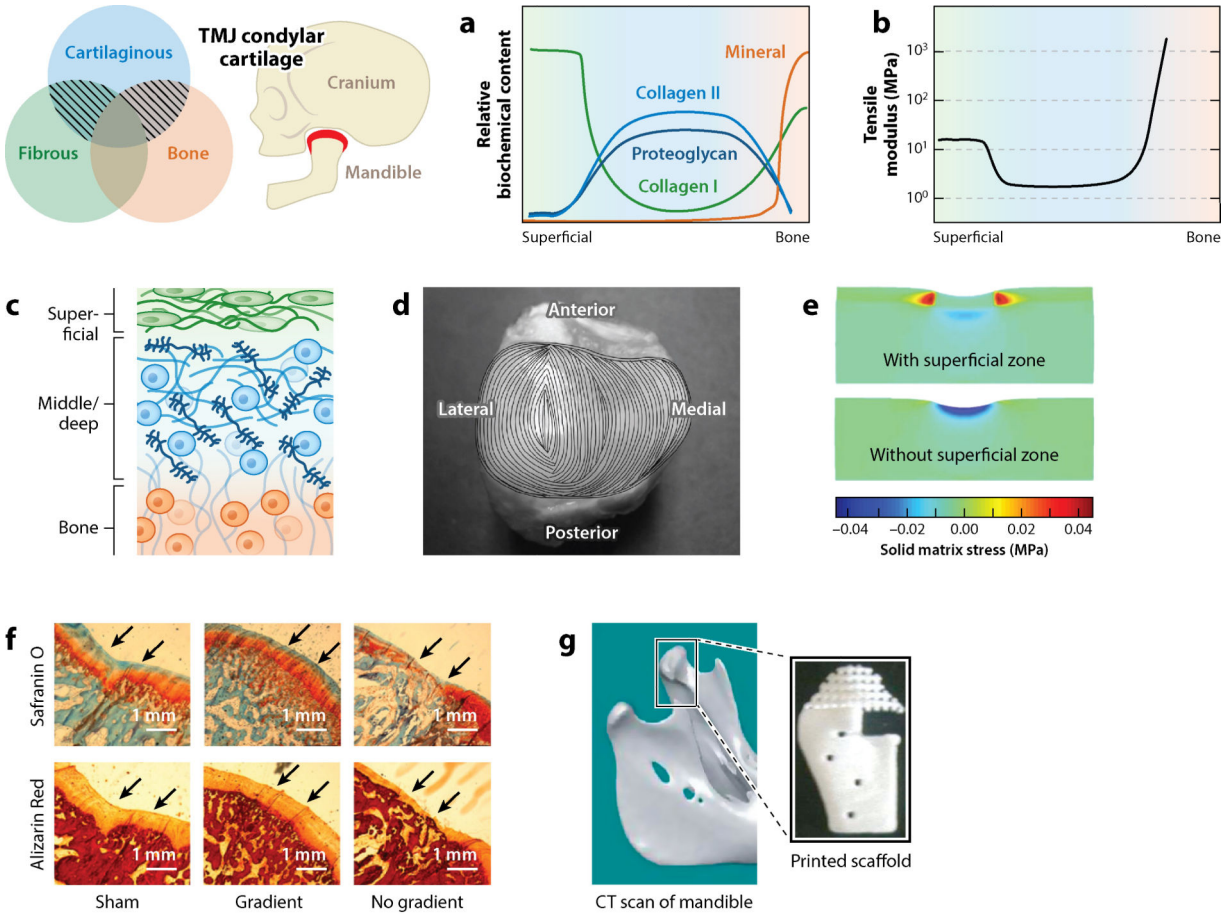

Figure 6.

The cartilage of the temporomandibular condylar cartilage (TMJ; *highlighted in red*) is distinct from typical articular cartilage due to the inclusion of a prominent fibrous superficial zone. This tissue exhibits (*a*) a biochemical gradient and (*b*) a mechanical profile where (*c*) a fibrous (*green*) type I collagen–rich superficial zone is stiff in tension compared with the cartilaginous middle and deep zones (*blue*), which then transition to comparatively rigid bone (*orange*). (*d*) The superficial zone exhibits location-dependent orientation and maintains a defined anterior–posterior orientation of type I collagen fibers. (*e*) Model-based evidence suggests that the increased tensile properties of the superficial zone shield the deeper cartilaginous tissue from elevated matrix stresses. (*f*,*g*) Efforts to engineer the TMJ condylar cartilage include methods to produce defined biochemical gradients in engineered composites (111). (*f*) Dormer et al. (111) revealed that introducing a gradient of biochemical cues within a tissue-engineered construct promoted both cartilage (Safranin O) and bone (Alizarin Red) formation. (*g*) Hollister et al. (112) focused on the reconstruction of the mandible using three-dimensional (3D) printing techniques. Abbreviation: CT, computed tomography. Panel *d* adapted from Reference 10 with permission. Panel *e* adapted from Reference 9 with permission. Panels *f* and *g* adapted from References 111 and 112, respectively, with permission.

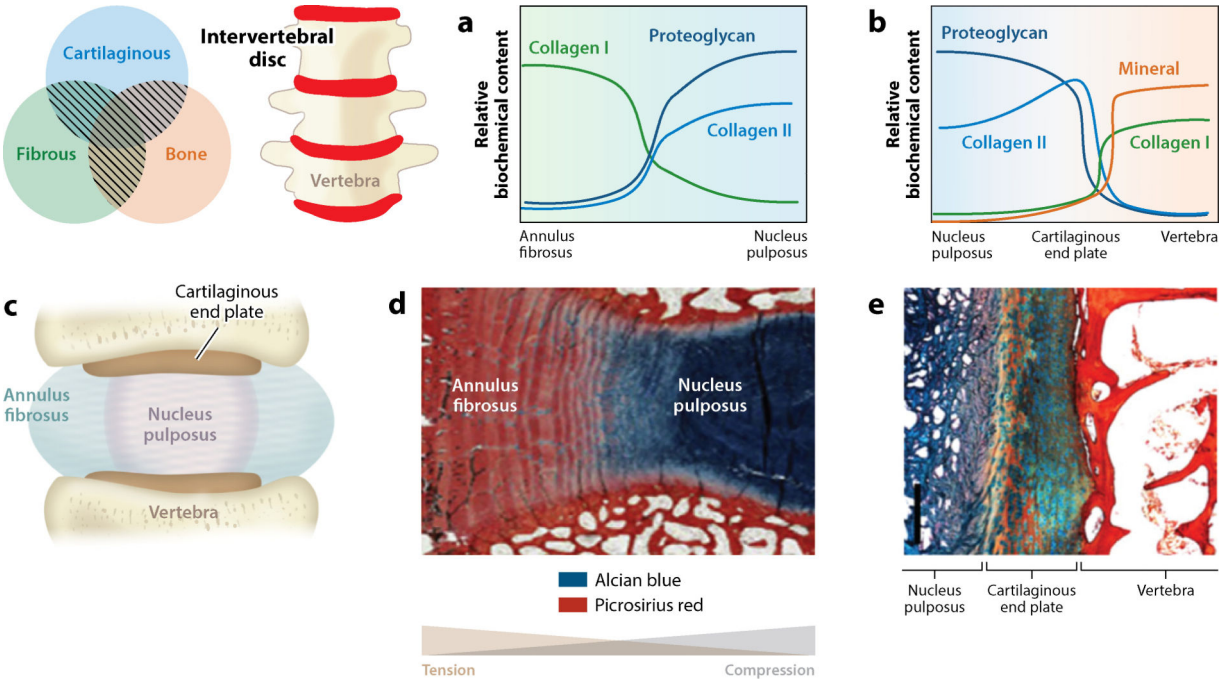

Figure 7.

The intervertebral disc maintains a composite graded structure with connections among cartilaginous, fibrous, and bone tissues. Variation in material connections exists along orthogonal axes. In the coronal plane schematic (*c*), the inner region of the disc, the nucleus pulposus (NP), has a gel-like morphology that is rich in proteoglycans. This region transitions to a dense fibrous tissue at its lateral periphery, the annulus fibrosus (AF). In the superior and inferior directions, the NP transitions first to a cartilaginous end plate, which then transitions to bone. The transition from AF to NP maintains (*a*) gradations in tissue compositions that relate to (*d*) location-dependent loading patterns. Due to the composite makeup and ordered structure of the disc, the NP experiences compressive loading whereas the AF experiences tensile loading. As the NP transitions to cartilage and then to bone, there also exist gradations in (*b*) biochemical makeup and (*e*) structure. Panel *d* adapted from Reference 129 with permission. Panel *e* adapted from Reference 130 with permission.

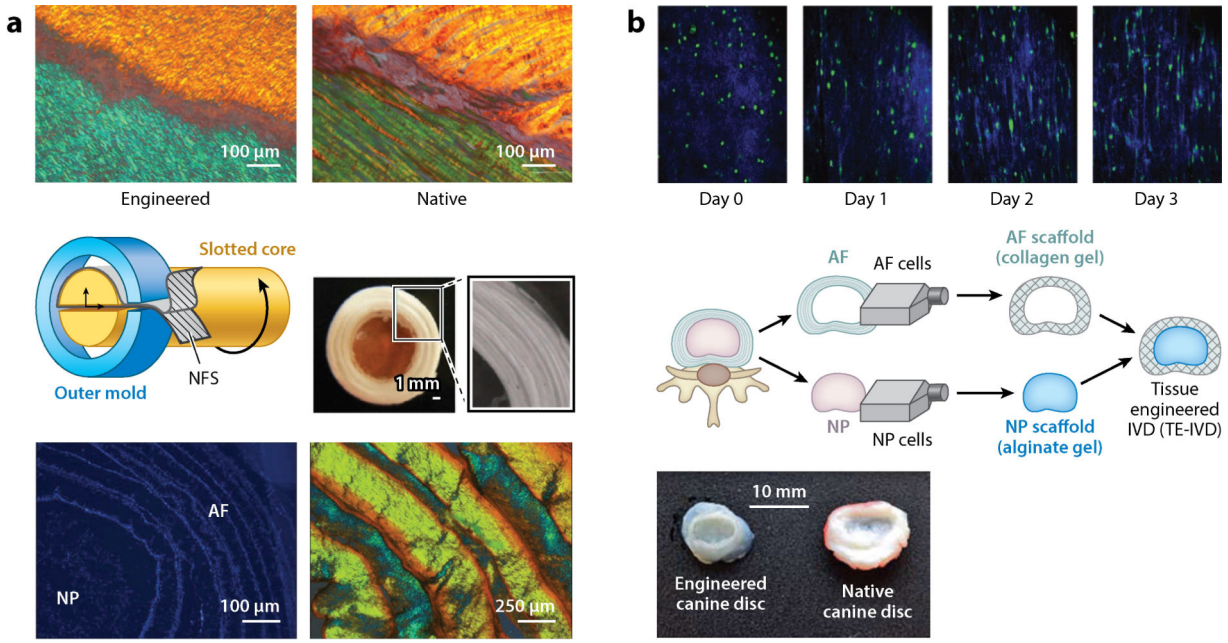

Figure 8.

(*a*) (*Top*) Creating layered sheets of electrospun nanofibrous scaffolds (NFS) recapitulates the lamellar collagen structure of the native annulus fibrosus (AF), maintaining the angle-ply structure as revealed by polarized light microscopy. (*Middle*) By winding these NFS into multilayer lamellar structures, and incorporating this engineered AF tissue with a central hydrogel, Nerurkar et al. (137) developed disc-like composite structures. (*Bottom*) Following culture, microscopy techniques revealed that cells remain viable and deposit substantial extracellular matrix, leading to native disc-like structure and function. (*b*) (*Top*) Bowles et al. (152) demonstrated that discs formed through cell-mediated, self-assembled collagen compaction show collagen and cellular reorganization around the nucleus, reminiscent of the aligned fibrous structure of the AF. (*Middle*) Through the incorporation of both AF and nucleus pulposus (NP) cells in a tissue engineering approach, disc-like composites have been fabricated by allowing a collagen gel to contract around an inner alginate gel core. (*Bottom*) Moriguchi et al. (138) showed that this technique can recapitulate the structure of canine discs. Abbreviation: IVD, intervertebral disc. Panel *a* adapted from References 137 and 150 with permission. Panel *b* adapted from References 138 and 152 with permission.